Accepted Manuscript

Geochemistry of groundwater in the Saint-Édouard area, Quebec, Canada, and its influence on the distribution of methane in shallow aquifers

G. Bordeleau, C. Rivard, D. Lavoie, R. Lefebvre, X. Malet, P. Ladevèze

PII: S0883-2927(17)30362-1

DOI: 10.1016/j.apgeochem.2017.11.012

Reference: AG 3994

To appear in: *Applied Geochemistry*

Received Date: 6 May 2017

Revised Date: 22 November 2017

Accepted Date: 23 November 2017

Please cite this article as: Bordeleau, G., Rivard, C., Lavoie, D., Lefebvre, R., Malet, X., Ladevèze, P., Geochemistry of groundwater in the Saint-Édouard area, Quebec, Canada, and its influence on the distribution of methane in shallow aquifers, *Applied Geochemistry* (2017), doi: 10.1016/j.apgeochem.2017.11.012.

Geochemistry of groundwater in the Saint-Édouard area, Quebec, Canada, and its influence on the distribution of methane in shallow aquifers

Bordeleau, G.*[a], Rivard, C.[a], Lavoie, D.[a], Lefebvre, R[b]., Malet, X.[a], Ladevèze, P.[a,b]

[a]Geological Survey of Canada, Natural Resources Canada, Quebec City, QC, Canada

[b]Institut national de la recherche scientifique (INRS), Quebec City, QC, Canada

Abstract

Shale gas and tight oil production has undergone a tremendous increase in the last decade in North America, which was accompanied by animated scientific debate and local public uproar concerning environmental issues, especially the risks of contamination for shallow groundwater resources. In Québec (eastern Canada), public concerns led to a *de facto* moratorium on hydraulic fracturing in 2010 for the St. Lawrence Lowlands, where the underlying Utica Shale is known to contain significant gas resources. As only a few exploration gas wells have been drilled, this vast area may still be considered "virgin". In 2012, a 4-year project was initiated by the Geological Survey of Canada, which aimed at characterizing aquifer vulnerability to deep industrial activities in the Saint-Édouard region, located close to Quebec City in the St. Lawrence Lowlands. As part of this project, a baseline study of hydrocarbons and other geochemical parameters was conducted in shallow aquifers. This paper presents groundwater geochemical characteristics in the region and assesses the geological, hydrogeological and geochemical controls on methane distribution.

Results show that methane is present in 96% of the 48 sampling points over the 500 km^2 study area, and that concentrations are highly variable (from undetected (<0.006 mg/L) to above 80 mg/L), sometimes over short distances and through time. Methane concentrations appear to be related to bedrock geology and to specific hydrogeochemical conditions, such as those found below the active groundwater flow zone (0-30 m within bedrock), where relatively old, chemically evolved water is found under semi-confined to confined conditions. Two main fault zones are well documented in the area, and there is clear evidence that some deep formation brines, in addition to marine water originating from the Champlain Sea, are migrating into shallow aquifers in the vicinity of one of them. This saline groundwater contribution is

attributed to the regional groundwater flow coming from the Appalachians and discharging along this normal fault zone close to the St. Lawrence River. The depth from which the brine originates is, however, unknown, but should not exceed a few hundred meters, as there is no indication that deep thermogenic gas from the Utica Shale is currently reaching the surface, through this pathway or elsewhere in this region.

Keywords: methane; baseline; Utica Shale; shale gas; formation brine

Corresponding author: genevieve.bordeleau@canada.ca

1 Introduction

Production of shale gas and tight reservoir hydrocarbons has undergone a tremendous increase in the last decade in North America, due to improvements in production techniques (Jarvie, 2012a; 2012b). The targeted geologic formations generally contain thermogenic gas and various proportions of liquid phases, which were formed under burial conditions of high temperatures. In the early phases of development, shale plays have been exploited for their dry gas content (essentially methane), such as that found in the Barnett (Texas), Haynesville (Louisiana, Texas), Fayetteville (Arkansas), as well as Marcellus and Utica (Pennsylvania and West Virginia) shales in the U.S. and in the Horn River (British Columbia) and Albert (New Brunswick) formations in Canada. However, due to the current low price of natural gas, mostly plays with associated liquids have been further developed in the past few years. Some of the most important shales that contain wet gas (essentially ethane, propane and some longer chain hydrocarbons) include the Eagle Ford (Texas) and Utica (Ohio) shales in the U.S. and the Montney (British Columbia) and Duvernay (Alberta) formations in Canada. In contrast, microbial (or commonly called biogenic) methane is produced by methanogenic microorganisms closer to the surface under anoxic conditions (Whiticar et al., 1986). Shales containing methane generated dominantly by microbial activity can also be commercially viable, such as the Antrim Shale (Michigan) in the U.S.

Thermogenic petroleum is entrapped within the tight pores of the shale matrix, which must be fractured (or "fracked") in order to release the petroleum that is then recovered in the production well (Rivard et al., 2014; Vidic et al., 2013). Please note that in this paper the term "shale" is not used under its strict definition. Indeed, shale gas and oil refers herein to a continuum of impermeable, fine grained lithologies (shale, mudstone, siltstone and very fined-grained sandstone) where hydrocarbons produced in the shale are stored *in situ* or in the interbedded lithologies (Jarvie, 2012b). The most common technique to fracture low-permeability rocks is hydraulic fracturing, which uses a mixture of water, proppants (generally sand) and chemical additives that are injected at high pressure, generally in horizontal wells in a variable number of individual stages or fracturing events. The advent of fracking technology has

caused much debate and concerns among scientists and the public on the environmental risks that these unconventional resources exploration and development activities pose, especially to groundwater quality (Lefebvre, 2017). For this reason, some jurisdictions such as New Brunswick and Nova Scotia (Canada) and New York (U.S.) decided to impose a moratorium on high-volume hydraulic fracturing, at least until the risks for drinking water resources are better defined and understood, and social acceptability is reached. The province of Quebec has had a *de facto* moratorium on fracturing for the St. Lawrence Lowlands since 2010, but a new regulation on water extraction and protection now specifying a regulatory framework for hydrocarbon exploration and exploitation activities was adopted in September 2017 (MDDELCC, 2017). This context (i.e. a period of a few years without oil and gas activities), has provided an opportunity to carry out environmental scientific studies that shed light on the environmental issues related to unconventional hydrocarbon development (Considine et al., 2012; Kennedy and Drage, 2015; Loomer et al., 2016; Moritz et al., 2015; Nowamooz et al., 2015; Pinti et al., 2013; Siegel et al., 2016).

Although fracturing has caused much public concern, it is now commonly accepted in the scientific community that the main risks to groundwater quality stem from: 1) the handling and treatment of drilling and fracking fluids as well as flowback water from the well, which can be accidentally spilled or otherwise stored in improperly sealed reservoirs at the surface (Vengosh et al., 2014; Lefebvre, 2017), and 2) fluid migration from depths through improperly-cemented gas well casings (Darrah et al., 2014; Jackson et al., 2013b). The incidence of these two contamination pathways can be minimized through the implementation of better industry practices and stricter regulations (Dusseault and Jackson, 2014), and several jurisdictions are starting to implement monitoring programs for drinking water wells located within a certain distance of shale petroleum wells, in order to detect contamination coming from the well or from development-related activities in the immediate vicinity (e.g., Boyer et al., 2012, MDDELCC, 2017). However, a third contamination pathway is possible, namely the upward flow of gas, fracking fluid and/or saline formation water through preferential migration pathways, either natural (faults or fractured zones), man-made (reactivated faulted zones or decommissioned or abandoned oil and gas wells) or a combination of both. Although a

potential fluid migration pathway through faults has been considered by expert panels (CCA, 2014; EPA, 2012) and has been suggested by some authors based on groundwater chemistry data (Révész et al., 2010; Warner et al., 2012), it has truly only been studied through numerical modeling (e.g. Gassiat et al., 2013; Kissinger et al., 2013; Reagan et al., 2015), and some researchers argue that such a process is unlikely (Dusseault and Jackson, 2014; Flewelling and Sharma, 2015). More details are provided in Lefebvre (2017).

While shallow aquifers are separated from the targeted shale unit by often more than 1500 m of low-permeability rock, possibilities of upward flow through this intermediate zone toward fresh-water aquifers are practically limited to fault zones having very particular conditions. Nonetheless, fluid migration from various depths into shallow aquifers through preferential pathways is still possible and was suspected in the context of various field studies (Allison, 2001; Bair, 2010; Li et al., 2016; Molofsky et al., 2013; Révész et al., 2010; Warner et al., 2012). If gas and other fluids migrate upwards through faults or fractures that are naturally permeable, or that are currently sealed but could potentially be reactivated through fracturing, these fluids could show up in aquifers at greater distances from the well heads than would be expected if contamination occurred through the gas well casing itself. Of note, thermogenic methane in groundwater can also originate from shallower, methane-rich (coal or shale) bedrock units in which the water circulates, such as in Pennsylvania (Marcellus Shale; Molofsky et al., 2013) or the St. Lawrence Lowlands (Lavoie et al., 2016).

To better understand the origin of the methane found in groundwater, the scientific community is widely calling for baseline groundwater characterization of targeted regions before unconventional hydrocarbon exploitation begins (Jackson et al., 2013b; Vengosh et al., 2014), although there has not yet been a consensus on the extent, methods, or duration/frequency of sampling involved in such baseline studies. Without such proper baseline studies, it could be very difficult to conclude whether groundwater quality has been impacted by unconventional hydrocarbon development activities, especially since methane can be naturally present in shallow groundwater of many regions, and because natural methane concentrations can vary greatly in space and time (Rivard et al., 2017a).

The Upper Ordovician Utica Shale found in the St. Lawrence Lowlands (southern Quebec, eastern Canada), is known to contain important quantities of thermogenic gas (Chen et al., 2014). The potential of this formation was assessed from 2006 to 2010 through the drilling of 17 vertical and 11 horizontal wells, of which 18 were fractured and tested before implementation of the *de facto* fracturing moratorium in 2010. This relatively low level of activity (average 1 fractured well per 555 km^2) makes the area almost pristine with respect to shale gas exploration. Despite the lack of shale gas exploitation, locally high concentrations of dissolved methane have been reported in several drinking water wells (Lefebvre et al., 2015; Moritz et al., 2015; Pinti et al., 2013).

In 2012, a research project was initiated by the Geological Survey of Canada, which aimed specifically at assessing aquifer vulnerability in an area of the St. Lawrence Lowlands that showed great potential for shale gas exploitation from the Utica Shale (Lavoie et al., 2014). The study area is centered around the municipality of Saint-Édouard-de-Lotbinière (henceforth called Saint-Édouard), located 65 km south-west of Quebec City. This area was selected because: 1) the Talisman Saint-Édouard #1 horizontal well (well A275) provided the most promising results for a production test within the St. Lawrence Lowlands; 2) it is a rural but relatively populated area where groundwater represents an essential water supply for residents and agriculture; and 3) several faults are known to be present in this area, which could represent preferential fluid migration pathways for deep fluids (Lavoie et al., 2014). Reports from Utica Shale oil and gas operators indicate that the reservoir is overpressured and that existing faults are sealed (Chatellier et al., 2013). However, while this suggests that surficial aquifers should not be connected to the deep Utica Shale, structural discontinuities could potentially alter these conditions (Séjourné et al., 2013).

This research project is multi-faceted and includes geophysical, geomechanical, hydrogeological, tectonostratigraphy and rock organic geochemistry aspects (Lavoie et al., 2016; Lavoie et al., 2014), in addition to an extensive groundwater geochemical study which is the subject of this paper. This multidisciplinary project thus innovates in attempting to identify multiple field evidence of preferential fluid pathways that could allow the migration of fluids

from shale gas horizons to shallow aquifers. The objectives of the present paper are to: 1) document the presence of dissolved methane in shallow aquifers of this region; 2) evaluate the influence of bedrock geology and groundwater geochemistry on the presence of dissolved methane; and 3) assess if there are geochemical indications of deep fluids migrating upwards into the shallow aquifers through fault zones, which could therefore represent preferential migration pathways for methane and other fluids related to eventual hydraulic fracturing. A thorough investigation of the origin of natural gas through a multi-isotope approach will be the subject of an upcoming paper.

2 Overview of published baseline studies

While numerous groundwater quality studies have been carried out throughout North America, the vast majority were conducted after large scale shale gas and tight oil exploitation had begun. This contributes to the difficulty of determining whether or not hydrocarbons found in groundwater are related to the oil and gas industry, which is reflected in the very different interpretations by various authors, from results obtained in the same region (Davies, 2011; Engelder, 2012; Jackson et al., 2011; Jackson et al., 2013a; Molofsky et al., 2011; Osborn et al., 2011; Saba and Orzechowski, 2011; Schon, 2011; Siegel et al., 2015a; Warner et al., 2012). Nonetheless, a few studies have been conducted prior to any large-scale fracturing activities in a few regions of the United States (New York, Pennsylvania) and Canada (Ontario, Quebec). These studies are reviewed in the present section.

In New York State, methane concentrations have been monitored as part of various general groundwater studies between 1999 and 2011 (Kappell and Nystrom, 2012). The highest concentrations were typically found in wells drilled in shale or in confined glacial unconsolidated aquifers overlying shale units. In a following study, McPhillips et al. (2014) found no significant correlation between methane concentrations and topography, distance from a conventional gas well, water wells installed in bedrock versus sediments, or geological units in which the bedrock wells were installed. Instead, methane concentrations were mostly

related to groundwater chemistry, with Na-dominated water types having the highest methane concentrations, as observed in a several other studies (Molofsky et al., 2013; Warner et al., 2012).

In Pennsylvania, a study compared groundwater quality before and after drilling and/or fracturing of 233 private wells located within 1.5 km of a Marcellus well pad (Boyer et al., 2012). The authors targeted both short-term (<8 months, but most sites <70 days) and longer-term (<26 months, but most sites <12 months) effects of drilling and/or fracturing, and analyzed general chemical parameters and methane. The authors reported no statistical difference in groundwater quality before and after drilling, except possibly for bromide at some locations. However, post-drill methane concentrations were only available for 48 out of the total of 233 wells. Siegel et al. (2015a; 2015b) used Chesapeake Energy's database containing several thousands of geochemical analyses from residential wells, mainly in Pennsylvania. The groundwater samples had been collected within the framework of baseline studies in the vicinity (< 1200 m) of proposed unconventional oil and gas well sites, prior to drilling. These authors also found no evidence of relationship between dissolved methane concentrations and proximity to oil and gas wells and no significant change in geochemistry before and after gas operations.

In Ontario, where the Upper Devonian Kettle Point Formation, Middle Devonian Marcellus Formation and Upper Ordovician Collingwood Member and Blue Mountain Formation represent potential future shale gas plays (Hamblin, 2006), McIntosh et al. (2014) studied the occurrence and origin of methane in groundwater using samples from 862 residential wells. The authors determined that methane in shallow aquifers was largely of microbial origin and that the highest methane concentrations were found in waters with distinct major ion geochemistry related to bedrock composition. A few samples showed evidence of mixing with basinal brines flowing upward into shallow aquifers, but these samples were generally not associated with high methane concentrations.

Pinti et al. (2013) and Moritz et al. (2015) published the first comprehensive regional study on alkane concentrations and isotopes in shallow aquifers of the St. Lawrence Lowlands of

southern Quebec. The eastern limit of their study area borders the western limit of our study area (see inset map on Figure 1). The authors report that methane was detected in 80% of the 130 sampled wells, with median, average and maximum concentrations of 0.1, 3.8, and 45.9 mg/L, respectively. The highest methane concentrations were found along the Yamaska normal fault, and the Logan and Aston thrust faults, with concentrations approximately 10 times higher than the average regional concentration, and isotopic values consistent with microbial gas. This suggests that faults could be preferential migration pathways for gas, but probably not from great depths. Immediately to the east of their study area lies the Chaudière-Appalaches region, where Lefebvre et al. (2015) (see inset map on Figure 1) have reported the presence of methane in 44 of 74 tested wells, with a median, average and maximum value of 0.2, 5.1 and 31.2 mg/L, respectively. Noteworthy, our study area is nested within that of Lefebvre et al. (2015), and some of the data was shared between the two projects. More specifically, the 74 wells for which they analyzed alkanes do include 20 of our wells. Conversely, in the present paper we include 11 of their wells (named INRS-xxx), some of which were resampled several times by our field crews over two years.

3 Site description

In the present study, we selected the small Saint-Édouard region located within the Chaudière-Appalaches region and conducted a high-density (approximately 10 times higher than the other regional studies in the St. Lawrence Lowlands) characterization of groundwater quality in residential and observation wells located within 30 km from the Saint-Édouard drilling pad. The spatial distribution of sampled wells, both for the visited residential wells and observation wells, was defined in order to cover the vicinity of the shale gas wells, the different geological formations and especially the fault zones between the shale gas wells and the St. Lawrence River. This also allowed us to define the groundwater quality along the groundwater flow direction.

3.1 Physiography and climate

The study area covers approximately 500 km^2 and is located 65 km south-west of Quebec City, on the south shore of the St. Lawrence River (Figure 1); it is centered around the municipality of

Saint-Édouard. The topography is rather flat, with slopes averaging around 2% (Lefebvre et al., 2015). Elevations are near sea level along the St. Lawrence River, and progress up to 160 m above sea level in the southeastern part of the study area, where the Appalachian Piedmont begins. Talisman Energy (now Repsol Canada) had drilled two wells in 2009 (one vertical and one horizontal; A267/A275) in the southern part of the study area, near the Appalachian domain (Figure 1). The horizontal well had been fractured at the beginning of 2010.

The climate of this region is humid and cold. Total precipitation is on average 1170 mm/y, of which 23% falls as snow. Mean monthly temperatures range from -11.7˚C (in January) to +19.8˚C (in July). There are nearly 40% of days with precipitation and 210 frost-free days.

3.2 Geology

Quaternary deposits are very heterogeneous both spatially and lithologically, reflecting the complex recent geological history of the region which has undergone several glacial-interglacial cycles, as well as a major marine episode, the Champlain Sea, which began some 13 000 years ago (in calendar years, not radiocarbon age) and lasted approximately 2 000 years (Occhietti, 2007). The sediments are mostly glacial and glaciomarine and are associated with the Champlain Sea (Lefebvre et al., 2015). Coarser alluvial and fluvioglacial deposits are also locally found; a map of quaternary deposits in the study area is available (Ladevèze et al., 2016).

The Paleozoic bedrock geology is divided into three domains, namely the autochtonous domain to the north, followed successively by the parautochtonous and allochtonous domains. The contact between the autochtonous and parautochtonous domains is defined by the easterly-verging backthrust Aston Fault, while a regional westerly-verging low-angle thrust fault known as Logan's Line separates the parautochtonous from the allochtonous domains (Lavoie et al., 2016).

The largest part of the study area lies within the St. Lawrence Lowlands, which belong to the autochtonous and parautochtonous domains of the St. Lawrence Platform. The stratigraphic units of these two domains are similar, with the parautochtonous domain being significantly more deformed with imbricated thrust slices (Comeau et al., 2004). The sedimentary succession

of both domains is composed of Middle Cambrian to Upper Ordovician shallow platform to ultimately deep marine rocks. In the autochtonous domain, the upper part of the succession is mainly constituted of grey-black shales and siltstones of the Nicolet Formation, which is part of the Lorraine Group, and of the Lotbinière Formation that belongs to the Sainte-Rosalie Group. In the parautochtonous domain, the upper part of the succession is mostly constituted of black calcareous shales of the Les Fonds Formation, which is also part of the Sainte-Rosalie Group (Globensky, 1987; Lavoie et al., 2016). The Lotbinière and Les Fonds formations are time and facies-correlatives to the Utica Shale, which can be found at a depth ranging from 500 and 2000 m between the north and the south of the study area (Lavoie et al., 2016). The St. Lawrence Platform strata are sub-horizontal and locally affected by mesoscopic open folds. High-angle normal faults displace in a staircase fashion the Precambrian basement and the St. Lawrence Platform succession up to the Utica Shale (Figure 2) (Castonguay et al., 2010; Séjourné et al., 2013). Previous geological interpretations (Castonguay et al., 2010; Konstantinovskaya et al., 2009) suggest that normal faults do not extend into the upper units of the Lorraine, Sainte-Rosalie and Queenston (found west of the study area) groups. A major normal fault is present in the northern part of the study area, namely the Jacques-Cartier River fault. It constitutes the eastern extension of the Yamaska Fault mentioned in Pinti et al. (2013); these authors have observed significantly higher methane concentrations along this fault and other regional faults, than elsewhere in their study area.

In the southern part of our study area, the Appalachian Piedmont belongs to the allochtonous domain, and contains sedimentary and volcanic rocks from the Cambrian to the Upper Ordovician (black shales with interbeds of clayey limestone, dolomite and siltstone), all of them highly deformed (Clark and Globensky, 1973; Lavoie, 2008). These transported deep marine rocks were put in contact with the St. Lawrence Platform units along Logan's Line during the Late Ordovician Taconian Orogeny (Tremblay and Pinet, 2016).

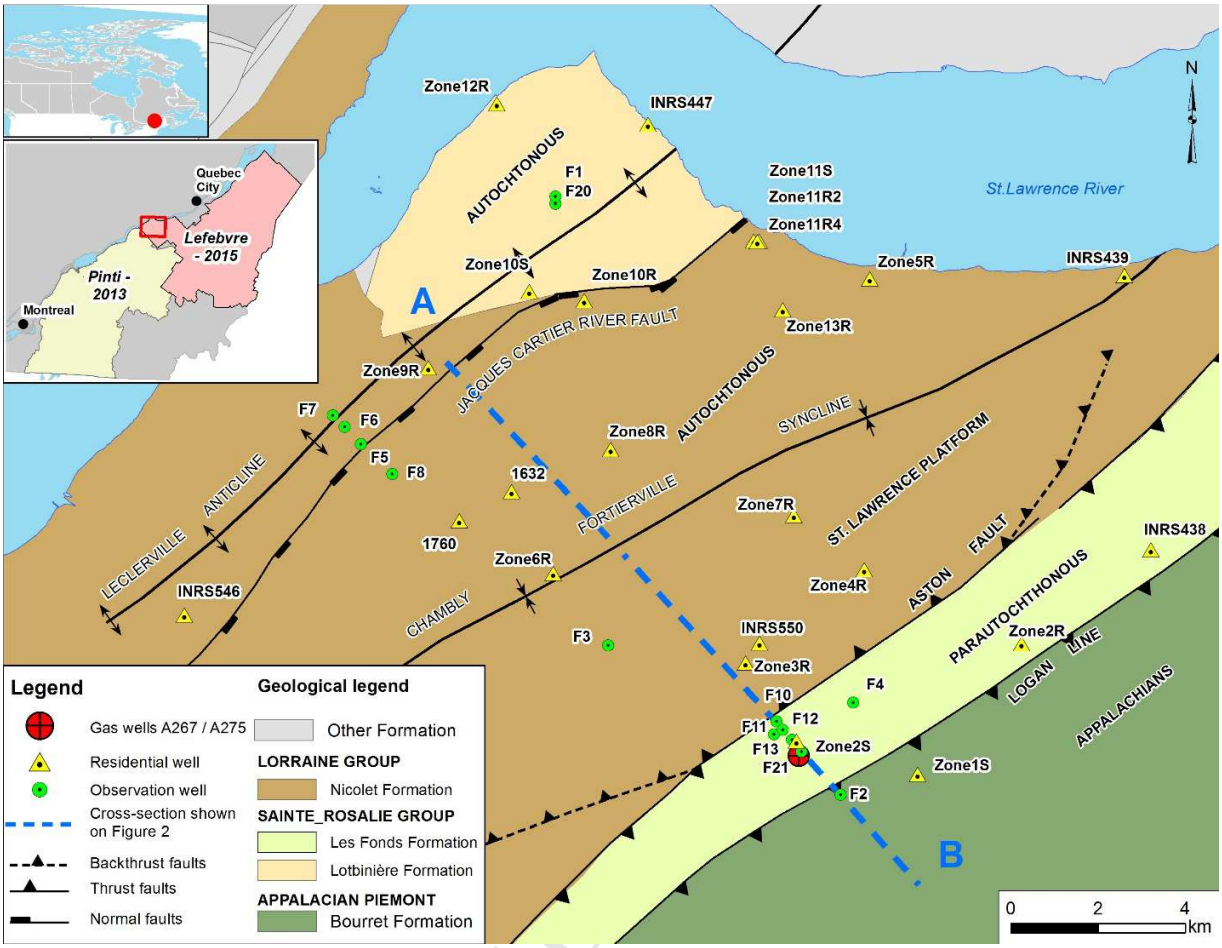

Figure 1. Location of the study area, including position of the sampled wells and bedrock geology. Wells A267 (vertical) and A275 (horizontal) are Talisman Energy exploration shale gas wells. The dotted line represents the cross-section shown on Figure 2. Inset map shows the extent of the study area (red rectangle) relative to those of Pinti et al. (2013) and Lefebvre et al. (2015).

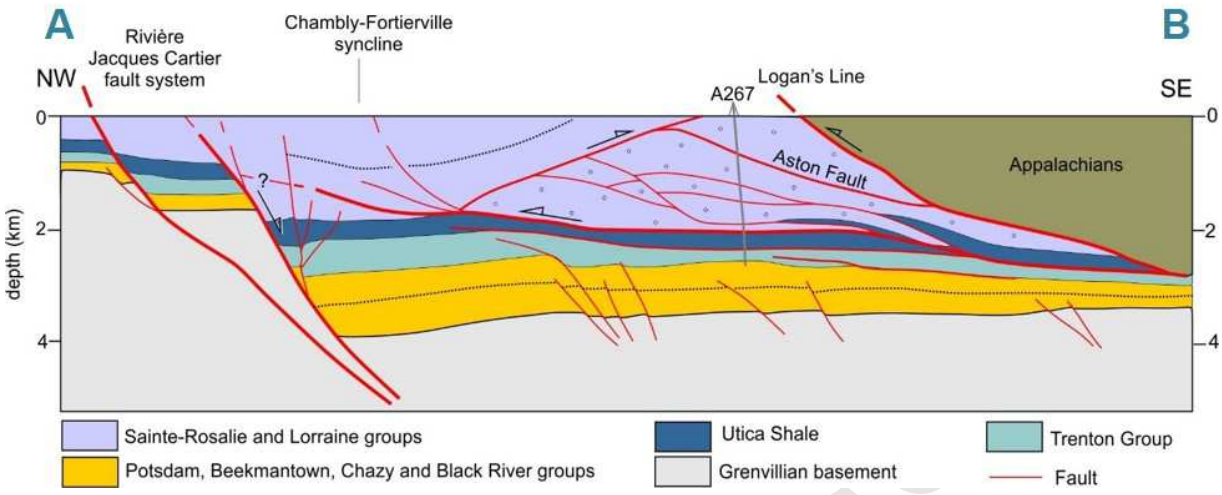

Figure 2. Geological cross-section of the Saint-Édouard area based on a seismic survey (taken from Lavoie et al., 2016). A and B correspond to the extremities of the cross-section shown on Figure 1.

3.3 Hydrogeology

Most of the study area is occupied by agricultural land. Although the bedrock permeability is low, most residential wells are exploiting this fractured rock aquifer, as the permeable Quaternary deposits that have a sufficient saturated thickness are very limited in extent. The Quaternary deposits are very heterogenous, and have been categorized by Ladevèze et al. (2016) into four distinct hydrofacies (HF1 to HF4), with hydraulic conductivities ranging from 10^{-8} to 10^{-4} m/s. At the location of the observation wells drilled for this project (see green dots on Figure 1), the thickness of the deposits varies between 0.9 and 40.8 m, with a median of 7.6 m and a prevalence of the lower conductivity hydrofacies (HF1 and HF2, 10^{-8} to 10^{-7} m/s) in most cases. The most permeable hydrofacies (HF4, 10^{-4} m/s) was observed locally in a few areas but was not present at the location of our observation wells. However, some of the municipal wells of Saint-Édouard, as well as some residential wells, are installed into this unit, which is the most productive in the region. Nonetheless, considering the sparsity of HF4, the mean hydraulic conductivity of the deposits over most of the study area is low to moderate. This results in a poorly permeable granular cover above the bedrock in many areas, leading to the presence of

confined or semi-confined conditions in the underlying fractured rock aquifer (Ladevèze et al., 2016). Another cause of the bedrock aquifer confinement or semi-confinement is the bedrock itself, which often contains unfractured intervals that confine the underlying aquifer intervals (Ladeveze, 2017).

Regionally, groundwater in the rock aquifer flows from southeast (Appalachian Piedmont) to northwest (St. Lawrence River). The confinement conditions were assessed in 10 observation wells by Ladevèze (2017) using different methods; results showed semi-confined (3 wells) to confined (7 wells) conditions. Aquifer conditions were not assessed for residential wells. Hydraulic conductivities of the bedrock were estimated using slug tests, with results spanning four orders of magnitude, from 10^{-9} to 10^{-5} m/s (Ladevèze et al., 2016). Conductivities are clearly higher in the Nicolet Formation (Lorraine Group, autochtonous domain), with values mostly in the order of 10^{-7} to 10^{-5} m/s, due to significant lithological intervals of fractured siltstone, especially in the northern part. In contrast, values in the Lotbinière and Les Fonds formations of the Sainte-Rosalie Group, and the Appalachian Piedmont (allochtonous domain), range from 10^{-9} to 10^{-7} m/s, due to the almost exclusive presence of calcareous black shale. Noteworthy, the highest hydraulic conductivities were found within a distance of 1 km to the north and south of the Jacques-Cartier River Fault. Borehole geophysics showed that for all bedrock units, flowing fractures are mostly located in the first 30 m of bedrock, suggesting a shallow active groundwater flow system (Ladevèze, 2017).

4 Methodology

4.1 General approach

The baseline groundwater characterization for the present study involved sampling shallow groundwater from a total of 30 residential wells, and 14 observation wells drilled for the project (15 wells were drilled but one remained dry throughout the study, likely located in fault gouge of the thrust fault zone). Among the 30 residential wells, 11 were borrowed from the Lefebvre et al. (2015) study, as mentioned in Section 2. Six of these 11 wells fall slightly outside of our

study area and are not visible on Figure 1, but they appear on a larger-scale map showing all sampling points in the Supplementary Information section (Figure S-2).

Among the 30 residential wells, four were surficial wells screened in unconsolidated sediments and 26 were open bedrock wells (Supplementary Table S-1). All observation wells drilled for the project were also open bedrock wells; their depth ranged from 30 to 147 m, with most being 50 m deep (Supplementary Table S-2). Four of the observation wells were sampled at two different depths (deep and shallow, separated by at least 25 m), bringing the total number of sampling points to 48 (30 residential + 10 single-depth observation wells + 4 double-depth observation wells).

All water samples collected for the first time at a given sampling point were analyzed for concentrations of major and minor ions and trace metals, dissolved inorganic carbon (DIC), dissolved organic carbon (DOC), as well as dissolved C_1-C_3 alkanes (methane, ethane and propane) and volatile organic compounds (VOCs). Concentrations of bicarbonate (HCO_3^-) and total dissolved solids (TDS), as well as water type, were computed using metal, ion and physiochemical data. Most of the wells were sampled between one and three times (subsequent samples were collected for a restricted number of compounds, notably alkanes and DIC). Seven wells were selected for a longer-term monitoring program; these monitoring wells were sampled between 11 and 18 times over a period of approximately 2.5 years. The specific results of the monitoring program regarding the variations in concentrations of targeted compounds over time and the impact of the sampling method are presented elsewhere (Rivard et al., 2017a,b). For the purpose of the current paper, the presented chemical results correspond to the geometric mean of analytical results for all samples collected at a given location.

Out of these 48 sampling points, some were also analyzed for isotopes aiming specifically at characterizing residence time within the groundwater flow system (tritium and radiocarbon, n=34; ^{36}Cl, n=2) or help interpret groundwater origin ($\delta^{18}O$ and $\delta^{2}H$, n=37).

4.2 Sampling techniques

Samples from residential wells were collected upstream from any water treatment system. The wells were purged until field physiochemical parameters (temperature, pH, dissolved oxygen (DO), redox potential (ORP), electrical conductivity) were stable over three measurements taken at 5-minute intervals. After purging, the flow rate was lowered to a minimum and a 6.25 mm (¼'') diameter tube was connected to the garden hose spigot to allow sampling with no water turbulence and minimal degassing.

Observation wells were sampled using a submersible pump, except for the deepest well. Either an impeller Redi-Flo2 submersible pump (Grundfos, Denmark) or a bladder submersible pump (Solinst, Georgetown, Ontario) was used, both with a 6.25 mm (¼'') tubing for water extraction. The pump was carefully lowered in the well until the desired depth, where the most productive fractures had previously been identified using downhole geophysical surveys (Crow and Ladevèze, 2015). In order to target water coming from the desired fracture zone, sampling was carried out at very low flow (below 500 mL/min, as recommended by the EPA, but usually <200 mL/min), to minimize drawdown in these low transmissivity wells. The median drawdown during sampling was 0.42 m, with a range from 0.01 to 3.58 m and a 90th centile of 1.30 m. In nearly all wells, purging was carried out until field parameters stabilized, which typically took between 0.5 and 2 hours. The exception is the "deep" samples collected from wells F3, F7 and F20, where the water that was targeted was the higher-TDS water located in the lower part of the wells. At some of these locations (F3, F7), purging resulted in rapidly decreasing salinity, as freshwater from the more permeable, shallower fractures was induced into the well. Therefore, these three samples were collected without purging. Also, the "deep" sample from our deepest well (F21, 147 m deep) was collected at a depth of ~145 m using HydraSleeve bags (https://www.hydrasleeve.com/) because none of our low-yield submersible pump could be lowered at this depth. Therefore, no purging was done, but the multiple bags (between 4 and 6) that had to be filled in order to collect the various samples showed that the physico-chemical parameters were similar for all bags. Careful comparison between these sampling methods showed they yield comparable results (Rivard et al., 2017b).

When sampling residential and observation wells, samples for most chemical analyses were simply poured into the appropriate bottles, after rinsing the bottles three times. For analyses of DIC, DOC, metals, and nutrients (ammonium (NH_4^+) and total phosphorus), samples were filtered using a 0.45 µm nylon membrane. Special care was taken to prevent degassing in bottles for C_1-C_3 concentrations and VOCs. For these analytes, the submerged container method was used, as recommended by the USGS (http://water.usgs.gov/lab/chlorofluorocarbons/sampling/bottles/). It is similar to the commonly used "inverted method" (Humez et al., 2016a; 2016b; Molofsky et al., 2016; Moritz et al., 2015; Siegel et al., 2015a), although the vial is kept in an upright position to avoid gas accumulation at its bottom.

4.3 Sample preservation and handling

Bottles/vials were kept refrigerated at all times. Preservation of samples for metals, nutrients, alkanes, and VOC analyses was ensured by the presence of acid in the bottles, resulting in a pH <2. Bottles for sulfides were preserved using zinc acetate and sodium hydroxide (NaOH). All sample preservation times prescribed by the laboratories were respected; samples for alkanes were always analyzed within 7 days of sampling, but the vast majority were analyzed within 2-3 days.

4.4 Analytical methods

Metals (Al, Sb, Ag, As, Ba, Be, Bi, B, Cd, Ca, Cr, Co, Cu, Sn, Fe, Li, Mg, Mn, Mo, Ni, Pb, K, Se, Si, Sr, Na, U, Ti, V, Z) and total phosphorus were analyzed using an Agilent (Santa Clara, CA) 7700X ICP-MS. Major ions (Br^-, Cl^-, NO_2^-+NO_3^-, SO_4^{2-}) were analyzed using a Dionex (Sunnyvale, CA) ICS-1600 ion chromatograph. Alkalinity and F^- were analyzed using a Mantech (Guelph, ON) PC-Titrate auto-analyzer. Sulfides were analyzed using a Thermo-Fisher (Waltham, MA) Evolution 60-S spectrophotometer, while NH_4^+ was analyzed using the Konelab Aqua 20 analyzer, also by Thermo Fisher. All these analyses were performed in a certified commercial laboratory (Maxxam Analytics, Quebec City, Canada).

Concentrations of dissolved C_1-C_3 alkanes were determined at the Delta-Lab of the Geological Survey of Canada (Quebec City, QC) using a Stratum PTC (Teledyne Tekmar, Mason, OH) purge and trap concentrator system interfaced with an Agilent (Santa Clara, CA) 7890 gas chromatograph equipped with a flame ionisation detector (GC-FID). The method employed was adapted from Pennsylvania Department of Environmental Protection method 3686 (PA-DEP, 2012) and US Environmental Protection Agency (EPA) method RSK 175 (Kampbell and Vandegrift, 1998). Detection limits on our samples were 0.006, 0.002, and 0.01 mg/L for methane, ethane and propane, respectively.

Water stable isotopes were analyzed using a Finnigan (now Thermo Fisher) MAT Delta plus XP + Gasbench at the G.G. Hatch Laboratory of the University of Ottawa, and results are presented in the usual delta (δ) notation expressed in per mil (‰) with respect to the international Vienna Mean Standard Ocean Water (VSMOW) reference. Precision is ±2‰ for δ^2H and ±0.15‰ for $\delta^{18}O$.

Tritium was analyzed by liquid scintillation counting at the University of Waterloo. For samples with conductivity > 5000 µS/cm, azeotropic distillation using toluene was performed before tritium analysis. Analysis of all samples was done using a PerkinElmer (Waltham, MA) LKB-WALLAC Quantulus 1220, after enriching 15 times by electrolysis. Results are expressed in tritium units (TU) and the detection limit and precision are 0.8 ± 0.8 TU.

Samples for ^{14}C analyses were prepared at the University of Waterloo and analyzed at the Direct AMS Laboratory (Accium BioSciences, Seattle, WA). Results are expressed in percent modern carbon (pmC) and are corrected to -25‰ $\delta^{13}C$-DIC. Analyses for $\delta^{13}C$-DIC were done at the University of Waterloo, using a Gilson (Middleton, WI) 222XL auto-sampler and a MicroGas-IsoPrime (Manchester, UK) mass spectrometer. The isotopic ratios are expressed in the usual per mil notation relative to the international Vienna Pee Dee Belemnite (V-PDB) standard. Precision is ± 0.2‰.

Finally, samples for ^{36}Cl analyses were prepared at INRS and sent to the Center for Accelerator Mass Spectrometry (CAMS) facility of the Lawrence Livermore National Laboratory for analysis. Results are expressed as the measured ratio of $^{36}Cl/Cl$ multiplied by 10^{15}, which will henceforth

simply be called "R^{36}Cl" $\left(R^{36}Cl = \frac{atoms^{36}Cl}{Cl} \times 10^{15}\right)$, and precision is within 1-3% of the reported value. Groundwater ages can be calculated using the ^{36}Cl half-life of 301,000 years, and taking into account the natural background ratio from cosmogenic and epigenic sources in recharge water for this geographic location (between 400 and 800; estimated based on values provided in Davis et al., 2000), as well as hypogenic ^{36}Cl production (estimated using values for shales and sandstone documented in Bentley et al., 1986). Complete details concerning calculations are found in the Supplementary Information section.

5 Results and discussion

5.1 General groundwater chemistry

The charge balance was verified for each sampling point by computing the concentrations (in meq/L) of major cations (Na^+, K^+, Ca^{2+}, Mg^{2+}) and anions (Cl^-, SO_4^{2-}, and alkalinity). The tolerance ((cations-anions)/(cations+anions)) was set at ±15%, which resulted in the rejection of only one residential well (Zone 10R). Moreover, while well INRS-547 had a satisfying charge balance of +1.3%, it was rejected because it appears to be strongly contaminated by de-icing salt (see Section 5.2). Noteworthy, out of the remaining 46 sampling points, 32 had a charge balance within ±5%, 11 were between ±5% and ±10%, and 3 were between ±10% and ±15%. Wells Zone 10R and INRS-547 were therefore not considered for statistical analyses related to water types, although they were kept for discussion on other parameters such as methane, salinity or groundwater age.

Based on the dominant cations and anions at each sampling point, four water types were defined for the region, namely Ca-HCO_3 (n=13, including the four wells in a granular aquifer), Na-Cl (n=6, plus well INRS-547 which contains de-icing salts), Na-HCO_3 (n=22), and finally Na-HCO_3-Cl (n=5, plus well Zone 10R). For the latter type, HCO_3 is the dominant anion but Cl^- represents ≥30% of the anions. Samples from this water type share a series of interesting characteristics, which will be discussed in the following sections. The Ca-HCO_3 type corresponds to "young" water that receives recent recharge, while the other types correspond to more

geochemically evolved water, with migration (residence) time likely increasing from Na-HCO_3 to Na-Cl (further discussed later).

The four water types are spatially dispersed throughout the study area and do not seem to follow a spatial distribution along the general groundwater flow direction (Figure 3). Water types are also unrelated to the different rock formations, and are rather mostly related to sampling depth, with Ca-HCO_3 water being typically associated with the shallowest depths (median of 18.3 m), followed by Na-HCO_3 (median of 26.7 m), then Na-HCO_3-Cl and Na-Cl (medians of 45.7 and 48.3 m, respectively) (Figure 4-A). Please note that for residential wells, pumps are normally positioned close to the bottom of the well, hence the sampling depth was assumed to be the same as total well depth. The four water types also exhibit different levels of TDS, with Ca-HCO_3 having the lowest values (median of 468 mg/L), followed closely by Na-HCO_3 (median of 554 mg/L), then Na-HCO_3-Cl (median of 1364 mg/L), and finally Na-Cl, with distinctly higher values (median of 3914 mg/L, with the highest value at 16 785 mg/L) (Figure 4-B).

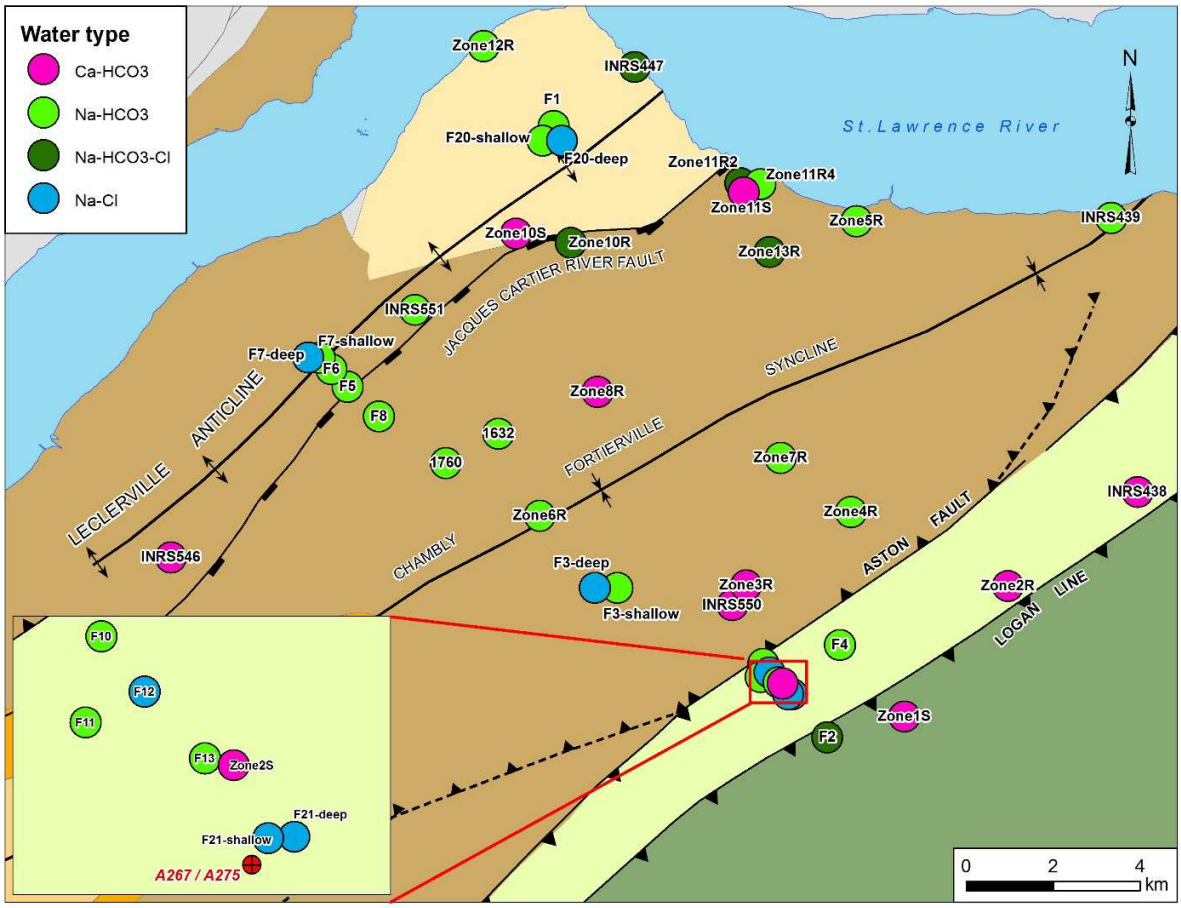

Figure 3. Spatial distribution of the four water types. Bedrock geology and other presented features are the same as on Figure 1.

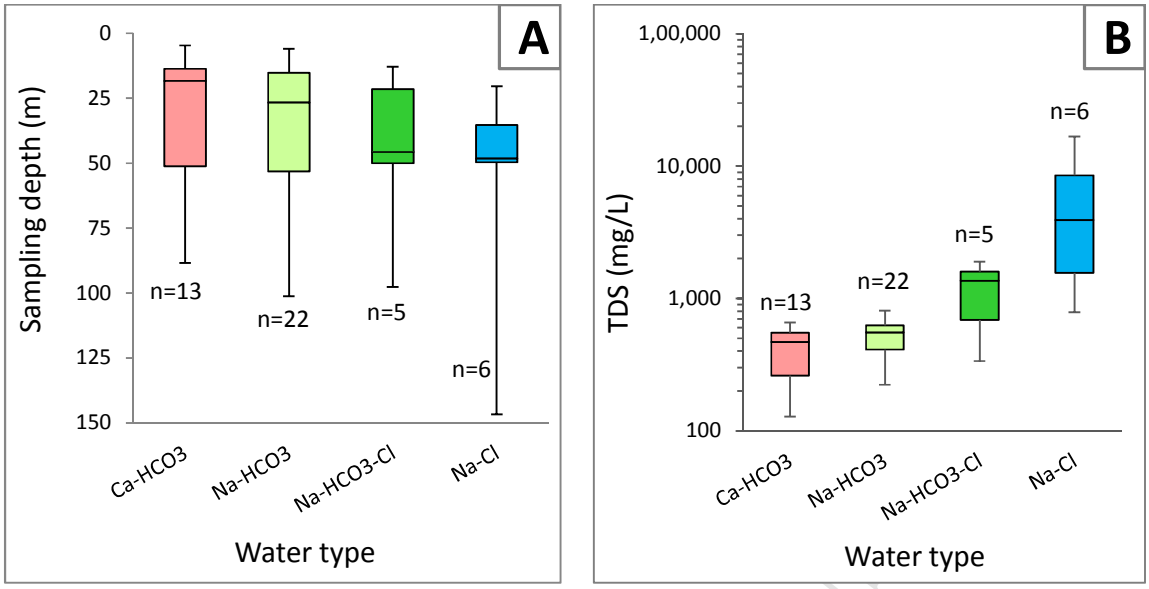

Figure 4: Sampling depth (A) and total dissolved solids (TDS) (B) for the four water types. Boxplot whiskers represent minimum and maximum values, box limits correspond to the 25th and 75th percentiles, while the central line corresponds to the median value.

5.2 Salinity

The source of salinity in our samples was investigated in order to: 1) identify potential mixing of waters from different origins, and 2) evaluate the possibility that deep, brackish or saline groundwater may be flowing upward and entering the shallow aquifers, which would indicate a connection between surficial aquifers and deeper strata.

The potential natural sources of groundwater salinity in southern Quebec are: 1) residual Champlain Sea water (Cloutier et al., 2010; Cloutier et al., 2008), trapped in Quaternary sediments or in the underlying bedrock during the 2000-year long invasion of this inland sea some 13 000 years ago; 2) deep formation brine (SIGPEG, 2017); and 3) evaporites (gypsum and anhydrite; Globensky, 1987). However, the presence of evaporites is quite sparse in the St. Lawrence Lowlands and restricted to the Queenston Group at the top of the sedimentary succession; this unit is not present in the Saint-Édouard area (Globensky, 1987). Potential

anthropogenic sources of salinity in the region include road salts, agricultural activities (fertilizers), and septic systems.

To constrain the origin of salinity, the bromide (Br^-) and chloride (Cl^-) concentrations from our samples were plotted, and compared to the average seawater value (Hounslow, 1995) and a seawater dilution line, and to formation brines. The brine samples on Figure 5-A to 5-C are from Junex gas wells Champlain #1 (sample from 645-750 m interval) and Junex Champlain #2 (sample from 502-850 m interval), both located approximately 50 km from our study area and taken from the Utica Group (SIGPEG, 2017). These are the closest formation brine samples available with suitable geochemical data. For these samples, Cl^- concentrations are available, but Br^- concentrations are not. A molar Cl/Br ratio of 200 was therefore assumed (see further in this section for related discussion).

The first feature that needs to be commented on Figure 5-A is the apparent horizontal alignment of samples at Br= 0.00063 mmol/L, which is an artefact due to the Br detection limit, as non-detects were assigned half the detection limit. Therefore for this group of samples, those to the left of the seawater dilution line do not provide information for the interpretation. In contrast, samples from the same "artefact" group, but located to the right of the seawater dilution line, definitely contain excess Cl^-; that is, considering their Cl^- concentration, they would need to contain detectable Br^- in order to be located along or above the seawater dilution line, which is not the case.

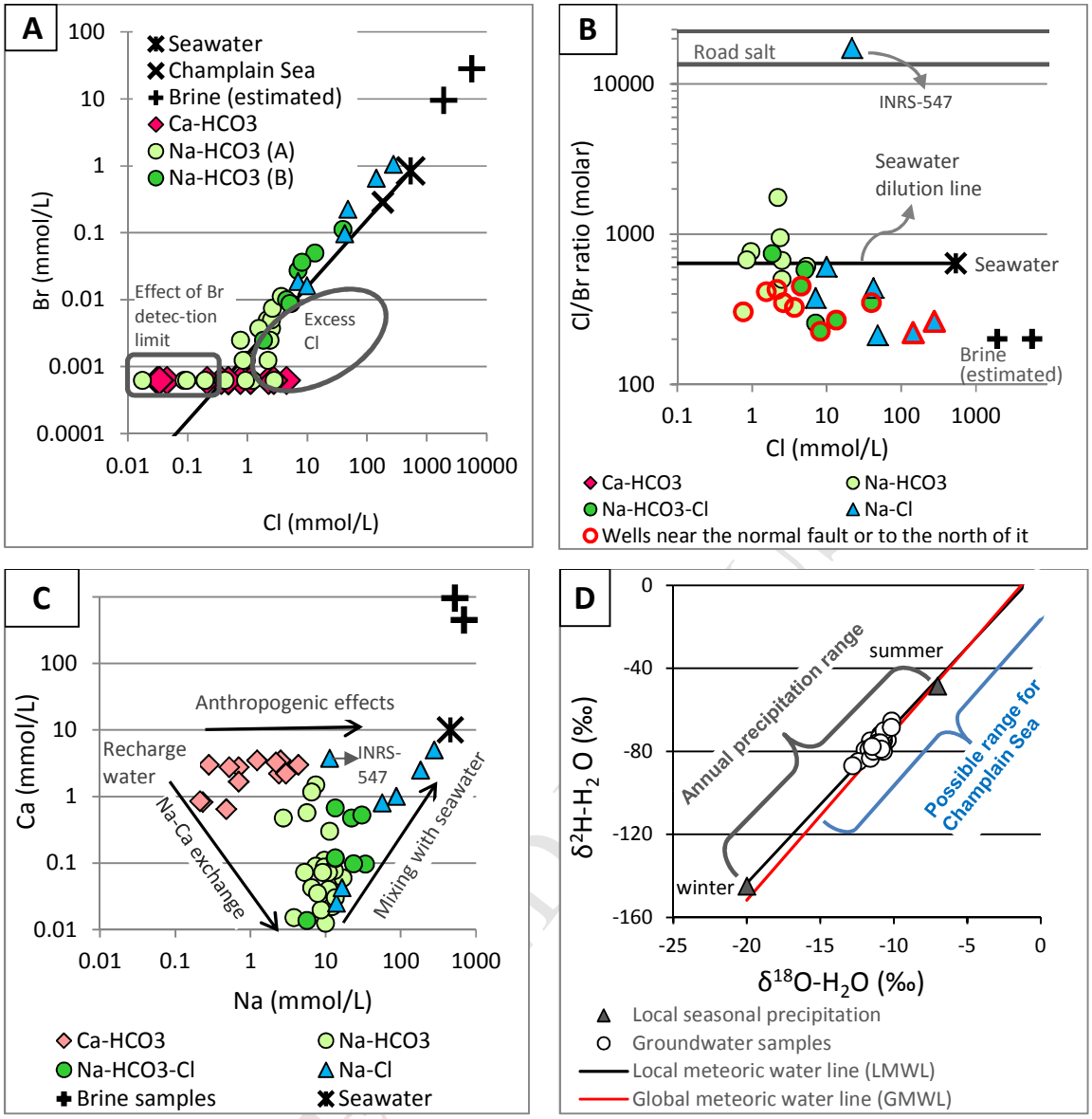

Figure 5: A) Concentrations of Br as a function of Cl; B) Cl/Br ratio as a function of Cl concentration; C) Ca as a function of Na; D) Stable isotopes of water in groundwater samples (this study) and precipitation (from Benoit et al., 2014), and possible range of values for Champlain Sea water (from Hillaire-Marcel, 1988).

All but one sampling points with excess Cl are within the Ca-HCO_3 or Na-HCO_3 groups, which are the water types representing the lower end of the groundwater evolution spectrum (i.e. the most recent), and are suspected to be the only water types that may be found under

unconfined conditions in the aquifer. As such, they represent water that may be more vulnerable to surface contamination compared to the other water types, and the excess Cl in these samples is likely due to anthropogenic activities. The main probable source of anthropogenic contamination is road salts, as all of these samples come from wells located next to a road where de-icing salts are used. Other compounds commonly associated with septic effluents or fertilizers, like nitrate/nitrite or phosphorus, are either undetected or are present at negligible concentrations in these wells (maximum value of 0.08 mg/L for P, and 1.1 mg/L for NO_3^-+NO_2^-).

In contrast, Na-HCO_3 samples collected in wells that are not along such roads fall either along or above (excess Br) the seawater ratio line. Interestingly, Na-HCO_3-Cl and Na-Cl samples from wells that are located along a main road do not contain excess Cl with respect to Br, which confirms that they are less vulnerable to surface contamination. The exception is well INRS-547, which has Na-Cl water containing the highest Cl excess of all samples, with a Cl/Br molar ratio of 17 354, compared to seawater which has a ratio of 639 (Hounslow, 1995). This well is located right next to a highway. The high amounts of salt used on the highway is most likely responsible for the salinity in this well, which is therefore not considered a true Na-Cl type and was excluded from the statistical analysis.

In Figure 5-A, there is also a series of points located along the seawater dilution line. The salinity in these samples can be explained by the presence of residual Champlain Sea water entrapped in the bedrock fractures, which is mixing with recharge water. All of these wells are completed in the Les Fonds formation or in the central or southern parts of the Lorraine Formation, therefore away from the Jacques-Cartier River fault.

Finally, there is a series of points that are located above the seawater dilution line, and which therefore contain excess Br^-. The excess of bromide may not seem to be significant in Figure 5-A due to the scale on the axes, but it is much more visible in Figure 5-B. These samples are all within the Na-HCO_3, Na-HCO_3-Cl and Na-Cl types, and most of them (identified by a red outline in Figure 5-B) are from wells located either in the vicinity of the Jacques-Cartier River fault (Lorraine Group) or to the north of that fault (Lotbinière Formation). This excess of bromide can

only be explained by a small contribution of another saline end-member, namely formation brines.

Calculations were made to estimate the proportion of the two saline end-members (brine and seawater) in samples. This was done for Na-HCO_3-Cl and Na-Cl samples only (n=12, thus excluding INRS-547), as they are not likely to be contaminated by road salts, which would otherwise add a third saline end-member. Calculations were based on the average Cl^- content of seawater (19 000 mg/L; Hounslow, 1995), the molar Cl/Br ratio of seawater (639; Hounslow, 1995), the average Cl^- concentration of the two aforementioned brine samples from industrial wells Junex Champlain #1 and #2 (134,000 mg/L; SIGPEG, 2017), and finally an assumed Cl/Br ratio of 200 for the brine. The latter is a best estimate, as Br^- concentrations for brine samples in this region were not available from the literature. However, Cl/Br ratios in basin brines are usually significantly lower than in seawater (Hounslow, 1995; Katz et al., 2011); for instance, Warner et al. (2012) found ratios in the order of 220-240 for Marcellus brines in northeastern Pennsylvania. In our study area, measured Cl/Br ratios in groundwater samples are as low as 213, hence the assumed ratio for the brine end-member had to be below this value.

The proportions of brine and seawater associated to the salinity in a sample ($f_{brine\ in\ salinity}$, $f_{sea\ in\ salinity}$), are calculated as follows:

$$f_{brine\ in\ salinity} = (R_{sea} - R_x) / (R_{sea} - R_{brine}) \quad \text{(eq. 1)}$$

$$f_{sea\ in\ salinity} = 1 - f_{brine\ in\ salinity} \quad \text{(eq. 2)}$$

where R_{sea} represents the molar Cl/Br ratio of seawater, R_x that of the groundwater and R_{brine} that of the brine.

The fraction (f) of brine contributing to the salinity of the Na-HCO_3-Cl and Na-Cl samples varies between 7 and 97% for the different samples, while the fraction of seawater varies inversely, i.e. between 3 and 93%. The resulting saline mixture is then diluted to different degrees with evolved meteoric water, resulting in the final salinity measured in the groundwater samples, such that:

$$f_{saline} = C_x / (C_{sea} \cdot f_{sea\ in\ salinity} + C_{brine} \cdot f_{brine\ in\ salinity}) \quad \text{(eq.3)}$$

where f_{saline} is the fraction of saline mixture in the sample, C represents the Cl^- concentration (in mmol/L) of the sample (x), seawater (sea) or brine (brine). The fraction of saline mixture in samples estimated using the values mentioned above varies between 0.2 and 8.3%, with the highest fractions observed near the Jacques-Cartier River fault or to the north of it.

From the fraction of saline mixture in a sample and the individual fractions of brine and seawater contributing to the salinity of the sample, it is possible to calculate the fraction of brine and seawater in samples; brine fractions in samples vary between 0.07 and 7.14%, while seawater fractions vary between 0.01 and 1.20%. These proportions will be compared to methane concentrations in Section 5.5. Noteworthy, the true Cl/Br ratio of the brine end-member could be somewhat lower than the assumed value of 200; however, the effect on the final computed fractions of brine and seawater in a sample would be relatively small. For example, if decreasing the assumed brine Cl/Br ratio from 200 to 100, the computed brine fractions in samples would be between 0.06 and 6.89%, and the seawater fractions in samples would be between 0.06 and 2.99%.

To infer evolution and mixing processes within the groundwater system, the relative abundance of calcium (Ca^{2+}) and sodium (Na^+) can also be used (Figure 5-C). Indeed, as precipitation enters the aquifer, the low pH of the water dissolves carbonate minerals, adding Ca^{2+} ions to the groundwater. Then, as groundwater evolution progresses, Ca^{2+} ions in the dissolved phase are exchanged for Na^+ ions that are adsorbed onto clay minerals of the aquifer material. The result is a gain of Na^+ and a loss of Ca^{2+} in groundwater in a two to one proportion, in accordance with the valence of the ions. Alternatively, Na^+ concentrations can increase without the accompanying decrease in Ca^{2+} as a result of anthropogenic contamination or seawater contribution, although in the latter case it is unlikely that recharge water would mix with old seawater without any evolution in between, in our study area.

In Figure 5-C, we observe a trend in our samples of increasing Na^+ concentrations accompanied by stable Ca^{2+} concentrations, mostly in the Ca-HCO_3 wells. This trend is interpreted as anthropogenic contamination, most likely by de-icing salts. In contrast, most Na-HCO_3, Na-

HCO_3-Cl, and Na-Cl samples are consistent with a path of natural groundwater evolution, i.e. starting with the composition of recharge water, then undergoing Na-Ca exchange (downward right direction, reaching the bottom of the graph when exchange is complete), followed by addition of seawater (upward right direction, towards the composition of seawater). In all of these samples, we observe near-complete Na^+ for Ca^{2+} exchange, followed by mixing with seawater to various degrees (Figure 5-C). A contribution of formation brines, which are expected to be enriched in Ca^{2+} due to secondary ion exchange reactions (Hounslow, 1995), is not apparent in our dataset.

5.3 Water stable isotopes

Water stable isotopes (δ^2H, $\delta^{18}O$) were measured at 37 sampling points and were compared to the global meteoric water line (GMWL; Craig, 1961), as well as the local meteoric water line (LMWL) established by Benoit et al. (2014) at a meteorological station located in Saint-Nicolas, approximately 30 km east of our study area. Values in groundwater vary between -65 and -87‰ for δ^2H, and between -10.2 and -12.8‰ for $\delta^{18}O$. All of the groundwater samples fall along the GMWL and LMWL, between the extreme values observed for winter and summer precipitation (Fig. 5-D). The groundwater values are consistent with the weighted mean annual values for local precipitation (δ^2H= -72‰, $\delta^{18}O$= -10.7‰); the average groundwater values for each of the four water types are similar, with type-specific average δ^2H between -77 and -79‰, and $\delta^{18}O$ between -11.1 and -11.5‰. This indicates that all groundwater samples are predominantly of meteoric origin.

This does not preclude the presence of a Champlain Sea component within our samples, however stable isotopic ratios of water cannot be used to detect it. Indeed, Champlain Sea water is thought to have had a $\delta^{18}O$ ratio between 0 (value for regular seawater) and -16‰ (reflecting estimated input of freshwater from glacial meltwater (-22‰) and Pleistocene stream water (-8‰) into the closed Champlain Sea (Hillaire-Marcel, 1977). The isotopic ratios in the Champlain Sea likely varied according to water depth, with deeper (more saline) water having isotopic values closer to normal seawater, and shallower water dominated by freshwater input from streams, precipitation and the melting Laurentian ice sheet (Hillaire-Marcel, 1988). To

illustrate the isotopic effect that a seawater component would have on groundwater samples, we consider a simple two-component mixing model involving pure seawater (δ^2H and $\delta^{18}O$= 0‰) and freshwater from modern recharge (corresponding to the weighed annual mean in local precipitation: δ^2H= -72‰ and $\delta^{18}O$= -10.7‰). This model is conservative, because: 1) it assumes that all of the chloride in samples is derived from seawater, which maximizes its isotopic effect, and 2) it does not consider the lower δ^2H and $\delta^{18}O$ values of the glacial meltwater and Pleistocene stream water, which could partly offset the higher isotopic values of seawater in remnants of the Champlain Sea. Despite this, results show that with the exception of three samples, the predicted range of isotopic values is contained within the actual range of values that were measured in groundwater samples, and within the range of modern precipitation. The exceptions are samples F7deep, F20deep and F21deep, which have the highest salinity in the region. The predicted isotopic values for these samples would reach up to -35‰ for δ^2H and -5.3‰ for $\delta^{18}O$. However, these are the samples with the highest proportion of deep formation brines contributing to their salinity (from calculations in Section 5.2) and hence, the actual isotopic effect of seawater should be much smaller than what is predicted from the simple model. While the δ^2H and $\delta^{18}O$ values of brines are unknown, their presence is not expected to be detectable using stable isotopes. Indeed, as noted by Warner et al. (2012), there are very large differences in ion concentrations between brines and freshwater, but smaller differences in stable isotopes. The result is that stable isotopes are not a sensitive tracer for the mixing of small amounts of brines into shallow groundwater.

5.4 Radioisotopes

Tritium and radiocarbon measurements were made at 34 sampling points, while ^{36}Cl analyses were done at two sampling points. ^{14}C-DIC values are shown in Figure 6 as a function of $\delta^{13}C$-DIC of the sample. As standard practice, values were normalized to a $\delta^{13}C$-DIC value of -25‰, which corrects for processes that modify the existing DIC and cause fractionation that affects both ^{13}C and ^{14}C. However, such standard correction has only a small effect on measured, uncorrected values (decreasing them by 0.02-1.55 pmC in our samples), and neglects the two main processes likely affecting the DIC in our study area, namely carbonate dissolution and

methanogenesis. Other reactions precursor to methanogenesis in the redox ladder, such as sulfate reduction, may also have similar effects (Clark and Fritz, 1997).

As calcite-undersaturated meteoric water percolates through the unsaturated zone and then circulates in the aquifer, it can dissolve Upper Ordovician marine carbonate minerals, which have a δ^{13}C-DIC of around 0‰ ± a few ‰ (Shields et al., 2003), and do not contain ^{14}C due to their old age (Clark and Fritz, 1997). If carbonate dissolution occurs under open system conditions in the unsaturated zone, the DIC added from carbonates will equilibrate with soil CO_2, thus acquiring a modern ^{14}C signature. In contrast, if carbonate dissolution occurs under "closed" conditions in the aquifer, the ^{14}C-free signature of carbonates will be retained, and the total DIC in the samples will be composed of two end-members: soil CO_2 with δ^{13}C-DIC= -25‰ and modern ^{14}C (≥100% pmC), and marine carbonates with δ^{13}C-DIC= 0‰ and ^{14}C= 0 pmC (Clark and Fritz, 1997). Most likely, a combination of both is occurring in our study area and globally, the dissolution may be assumed to occur under partially-open conditions, hence the samples containing dissolved carbonates will appear somewhat older than they actually are.

Methanogenesis is another process which may increase the δ^{13}C-DIC value of samples, while possibly (but not invariably) decreasing the ^{14}C values, as methane can either be produced from old and dead carbon present in the aquifer, or from more modern carbon in soils at shallow depths. The fractionation on the δ^{13}C-DIC occurs because methanogens first consume the isotopically lighter carbon molecules in their food source (acetate or CO_2, depending on the methanogenic pathway). Both methanogenic pathways result in an increase in the DIC concentration and δ^{13}C-DIC of the carbon pool (Clark and Fritz, 1997). If the groundwater system is closed or significantly restricted in terms of input of recent carbon, the δ^{13}C-DIC values can increase past 0‰ and values as high as +25-30‰ have been observed (Sharma and Baggett, 2011; Martini et al., 1998; Rivard et al., 2017a). Generally, values above +10‰ are considered to unequivocally show the occurrence of methanogenesis (Sharma and Baggett, 2011). The effect of fractionation will also be observed on the ^{14}C value, although the latter will largely be affected by the age of the carbon substrate used for methane production.

As explained, the two processes mentioned here cause an increase in δ^{13}C-DIC values: carbonate dissolution should result in δ^{13}C-DIC values not exceeding 0‰, while methanogenesis involves fractionation, which may increase the δ^{13}C-DIC much further (Figure 6-A). The observed effect of methanogenesis on the groundwater DIC pool depends on several factors, such as the relative importance of the two known methanogenic pathways (acetate fermentation versus CO_2 reduction), the size and original isotopic ratio of the carbon pool, the degree of "closeness" (confinement) of the groundwater system, the methane production rate, and the time elapsed since the onset of methanogenesis. These factors may vary spatially and some may also vary temporally, so quantifying them with a reasonable level of precision is a very complex task. The same is true about evaluating the relative isotopic effects of carbonate dissolution versus methanogenesis in our samples. Our data show that both processes are likely occurring in our study area, as illustrated by the apparent trend of points along the (closed-system) carbonate dissolution line, as well as the presence of several points exceeding +10‰ δ^{13}C-DIC (Figure 6-A). While quantitative correction of the ^{14}C values was not attempted, the data can still be used qualitatively to provide insight into groundwater characteristics of the different water types.

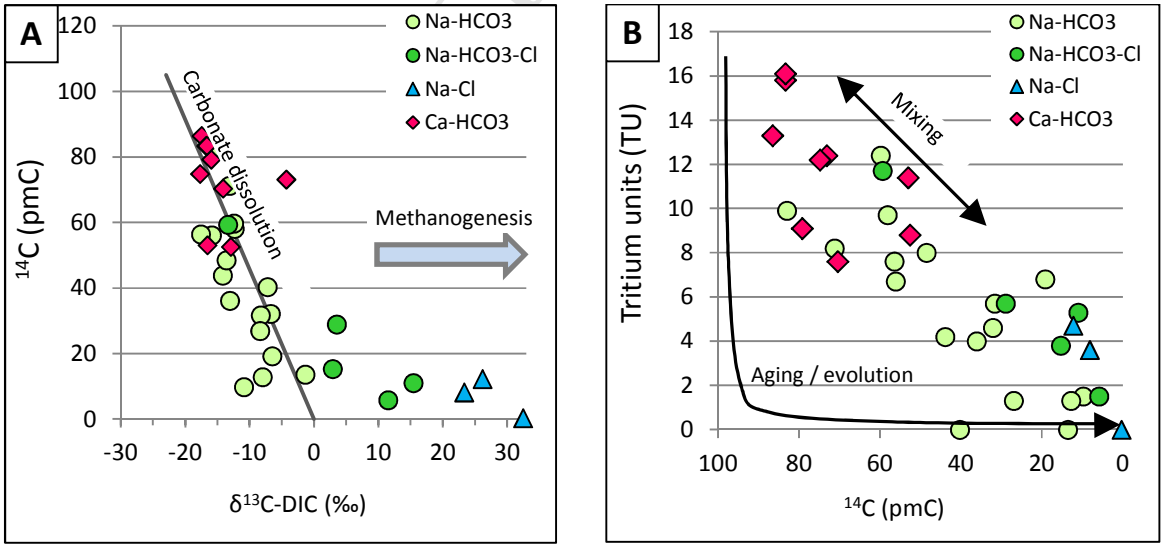

Figure 6: A) Radiocarbon as a function of δ^{13}C-DIC, and B) tritium as a function of

radiocarbon.

Ca-HCO_3 type samples contain between 53.0 and 86.5 pmC (Figure 6A), which may seem low for water collected in wells screened in shallow unconsolidated sediments or in shallow bedrock. However for this water type, methanogenesis is not likely to occur, as the redox conditions are not favourable: 1) aerobic conditions (DO >1 mg/L) are found in 5 out of 13 wells, 2) DO is detected, although below 1 mg/L, in 4 additional wells, and 3) redox potential values (with respect to standard hydrogen electrode, or Eh) vary between -73 and +674 mV. Knowing that methanogenesis does not come into play for this water type, taking into account the effect of carbonate dissolution results in values "sliding upward" along the carbonate dissolution line, bringing the original values towards modern values. This is not shown on Figure 6, as we wanted to keep comparable values for all water types.

Indeed, such correction would not be appropriate for the other water types, as methanogenesis likely influences the isotopic values in most samples. Nevertheless, it is clear that Na-HCO_3 water is older than water of the Ca-HCO_3 group and that Na-HCO_3-Cl and Na-Cl waters generally represent the oldest water within the study area (Figure 6-A). While all but one of the Na-HCO_3-Cl and Na-Cl samples have ^{14}C values below 30 pmC, it is clear that these samples are affected by methanogenesis, as $\delta^{13}C$-DIC values reach between +2.94‰ and +32.49‰. Elevated $\delta^{13}C$-DIC values such as those observed in Na-HCO_3-Cl and Na-Cl samples are only possible in a closed, or at least highly exchange-restricted reservoir, where input of freshwater and new carbon is very limited (Sharma and Baggett, 2011). This is consistent with the geochemical evolution stage of these water types, the absence of contamination by de-icing salts, and the low levels of detected tritium (Figure 6-B).

The amount of tritium detected in Na-HCO_3-Cl and Na-Cl samples is indeed generally much lower than in Ca-HCO_3 and part of the Na-HCO_3 samples, indicating that the radiocarbon content observed for each water type is not just an artifact of carbonate dissolution and/or methanogenesis, but rather reflects progressively increasing ages between water types. However, it is important to note that the actual presence of tritium in all but three samples

indicates the contribution to varying degree of a modern water component even within old, restricted reservoirs containing evolved groundwater. In fact, the combination of tritium and radiocarbon values in most of our samples clearly indicates mixing of different water sources rather than natural geochemical evolution, as shown in Figure 6-B.

The only samples with no detectable tritium are those from well F10, an artesian flowing well located along the Aston Fault, and from well F7 (both F7shallow and F7deep) located near the Jacques-Cartier River fault. In well F10, the absence of tritium is likely due to the upward flow conditions bringing older water into the well. This water has relatively low salinity (TDS 381 mg/L), a Cl/Br ratio close to that of seawater, and contains 13.57 pmC. In sharp contrast, sample F7deep (collected at 48 m depth) has the highest salinity of all samples (TDS 16 785 mg/L), a Br excess (molar Cl/Br ratio of 263), and is the sample containing the highest proportion of brine (7.14% of the sample according to calculations made in Section 5.2). Sample F7deep contains no measurable ^{14}C, and has a ^{36}Cl ratio of 9.25, which translates into an estimated age of 1.81 million years or older (see Supplementary Information for details). At this depth in the well, an upward flow gradient is observed, which can explain the infiltration of very old brine and absence of modern water. While the Jacques-Cartier River fault core is most likely sealed at the depth (500 – 2000 m) of the Utica Shale (Aguilera, 1978; Chatellier et al., 2013; Séjourné et al., 2013), it is possible that shallower fractures associated with this fault could be partially open and act as migration pathways for water containing marine water from the Champlain Sea and brines coming from a yet undetermined depth (probably less than 500 m). This fault zone would thus correspond to a discharge area for the regional groundwater flow. Brackish to saline water would discharge into the shallow aquifer in the vicinity of this fault zone and then follow the groundwater flow direction towards the north (St. Lawrence River), mixing with younger water along the way in the active groundwater flow zone (see Section 5.6 for more detail). This hypothesis is supported by sample F20deep, collected at a depth of 48 m in well F20, located 1.5 km north of this fault. This sample contains the second highest proportion of brine (TDS of 9884 mg/L, Cl/Br ratio of 221, estimated brine proportion in sample of 3.78%), some tritium (3.6 TU), some ^{14}C (8.17 pmC), and has a $R^{36}Cl$ of 11.07

(translating into an age of 1.73 million years or older). This indicates again mixing of very old groundwater with young water in the shallow aquifer.

5.5 Methane, ethane and propane

Concentrations of C_1 to C_3 alkanes (methane, ethane and propane) were measured at all sampling points and the data presented here correspond to the geometric mean of all C_1-C_3 results obtained at a given sampling point. While the geometric mean does not represent individual samples and does not underscore the variability of results at a given well, it was considered the best way to draw a representative portrayal of the methane concentration distribution in this region, notably by attenuating the effect of outliers at a given well.

Methane was detected in 46 out of 48 sampling points (96% of all sampling points), at geometrically-averaged concentrations ranging between the detection limit (0.006 mg/L) and 42.5 mg/L. Please note, however, that the concentration in individual samples for a sampling point could be higher and even reached as high as 82 mg/L in F21deep. Concentrations in several samples thus exceeded methane solubility at atmospheric pressure and groundwater temperature (~31 mg/L at p_{atm} and 10 ˚C temperature). However, groundwater samples were collected at depths reaching up to 147 m below ground surface, and the water level in all wells is within 10 m from the ground surface. Consequently, the sampling points are located from 4 to 140 m below the water level in wells, which results in higher methane solubility (solubility approximately doubles every 10 m due to the corresponding increase in pressure). Because water samples were rapidly lifted to the surface and collected using the submerged container method, partial exsolution may have occurred, but the sample did not have time to reach equilibrium before the bottles were capped, resulting in potential pressurization of the samples. This explains that some measured concentrations are above the theoretical solubility at atmospheric pressure. Due to exsolution, results above the saturation point at atmospheric pressure should be viewed as minimum concentrations present in the sample, rather than true concentrations found at the sampling point.

Over the entire study area, the median and (arithmetic) mean methane concentrations are 4.9 and 10.4 mg/L, respectively, which is much higher than the values found elsewhere in the St. Lawrence Lowlands (Lefebvre et al., 2015; Pinti et al., 2013). Figure 7 presents the spatial distribution of methane concentrations in the study area, using bedrock geology as background. This figure shows that methane is ubiquitous in the study area, concentrations do not follow a spatial distribution along groundwater flow lines, and high methane concentrations do not seem to be particularly localized near known faults. Very high (>20 mg/L) and low (<1 mg/L) concentrations may be found in any of the black shale-dominated geological formations present in the study area. The six "background" wells borrowed from Lefebvre et al. (2015) that are only visible on the extended version of the map (Supplementary Figure S-2) are located within non shale-dominated formations of the Appalachian Piedmont (succession composed of alternating shale and siltstone, dolomite and/or limestone). All of these have very low methane concentrations (<0.085 mg/L), except for well INRS-446 which is very close to the Les Fonds Formation, and has higher methane concentration (5.1 mg/L). There is no apparent correlation between methane concentrations and distance from the Talisman A267 and 275 gas wells (Figure 8-A). Instead, the presence of methane is mostly related to aquifer semi-confined or confined conditions, and to water type (Figure 8-B). The relationship between methane and topography was not tested, as most of the area is relatively flat.

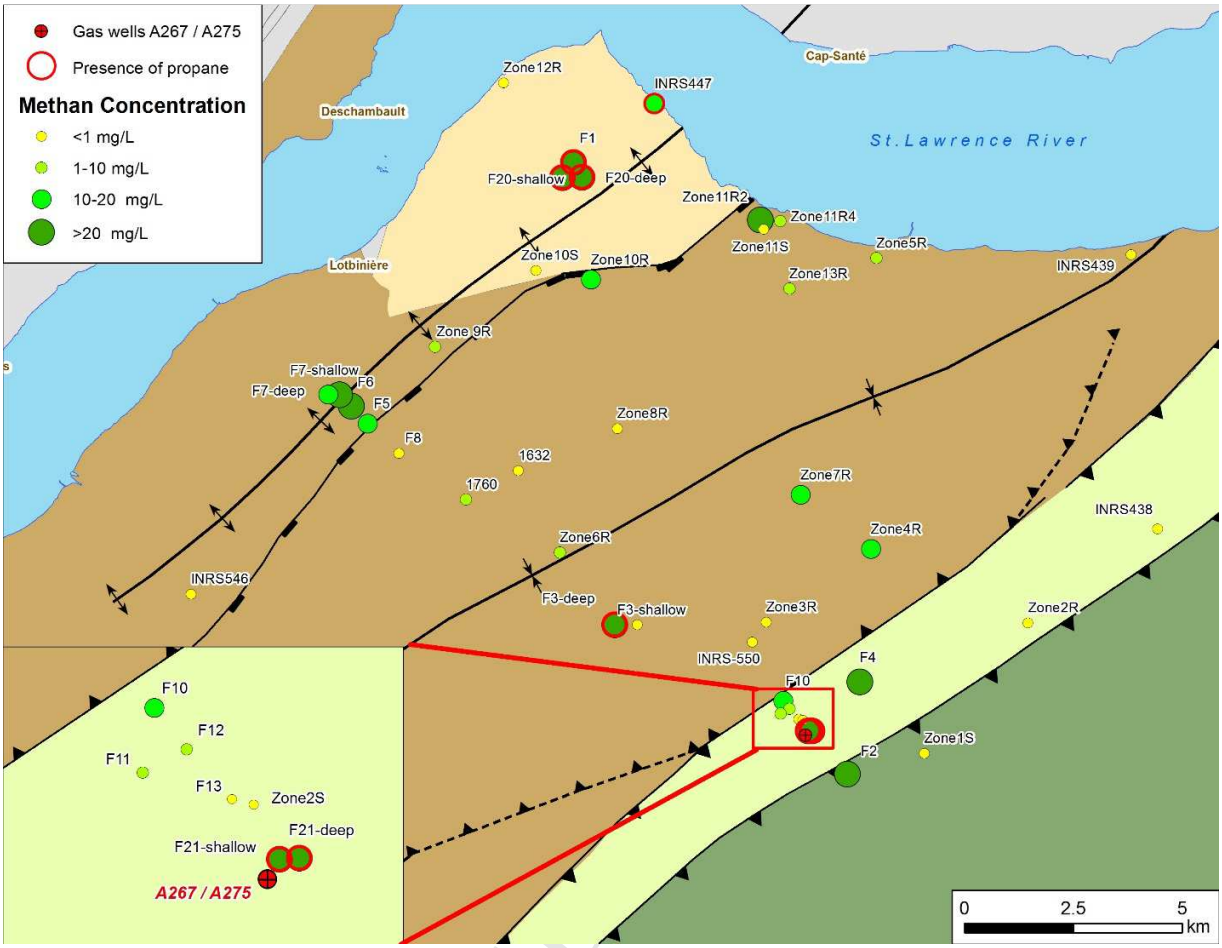

Figure 7: Distribution of methane concentrations in the study area (green circles). Samples containing propane are outlined in red (n=7). Well Zone 9R does not show a red outline, as propane was only detected in the first of 12 sampling events at this well. Bedrock geology and other features are described in Figure 1.

The relationship between methane and water type is in line with findings of other authors (McPhillips et al., 2014; Molofsky et al., 2013; Warner et al., 2012 among others). None of the averaged methane results for the Ca-HCO_3 samples exceeded 0.5 mg/L (Figure 8-B). While there is a marked difference in the median concentration of all water groups, with 0.08 mg/L for Ca-HCO_3, 4.4 mg/L for Na-HCO_3, 18.4 mg/L for Na-HCO_3-Cl, and 30.0 mg/L for Na-Cl, there is

considerable overlap between the ranges of methane concentrations found in the last three water types (Figure 8-B).

The fact that most Cl-dominated samples contain high methane concentrations does not imply, however, that deep brines are carrying along high methane concentrations. In fact, there is no clear correlation between methane concentrations and the estimated proportions of brine or seawater in samples (Figure 8-C). Moreover, high methane concentrations were not preferentially detected near the Jacques-Cartier River fault, where upward flow of some deep brine is inferred. Actually, sample F7deep (collected at 48 m depth and containing the highest proportion of old brine) has a lower methane concentration than sample F7shallow, collected at a depth of 17.7 m in the same well, and containing comparatively younger water. This confirms that methane is not directly related to the source of salinity.

Not surprisingly, a trend is observed between methane concentrations and the ^{14}C activity (Figure 8-D). While low methane concentrations may be encountered throughout the whole ^{14}C spectrum in our samples, high methane concentrations only occur in groundwater with low ^{14}C content and which is more evolved geochemically. Once again, this would be consistent with an old reservoir where input of freshwater and nutrients is highly restricted, and where redox conditions are favorable to methanogens. These methanogens can produce important amounts of methane, but very little ethane or propane (Davis and Squires, 1954; Vogel et al., 1982). The absence of ethane and propane in many of the samples with the oldest water may therefore give an indication that the observed gas could predominantly be of microbial origin. As mentioned above, the isotopic composition and origin of methane of these samples will be discussed in a future paper.

For ethane and propane, the geometric mean of all individual samples collected over time from a given sampling point was computed, like for methane. Based on this, ethane was detected in 18 sampling points, and propane in seven sampling points. None of these sampling points are in the Ca-HCO_3 group. Most of the detected ethane concentrations (11 out of 18) are negligible compared to methane (850 to 6500 times lower), which points towards microbial gas. Among the other samples, which contain more ethane (0.15-5.86 mg/L), all but one also contained

propane. Samples with propane are represented with a red outline in Figure 7; they are dispersed among the Lotbinière (4) and Les Fonds (2) formations and Lorraine (1) Group.

Except for one sampling point, the presence or absence of ethane and propane was consistent over time, and therefore the geometric mean of all individual samples provides a good representation of the situation. However, there is one sampling point (residential well Zone 9R), where the results were different in the first sampling event than in the 11 subsequent sampling events. Indeed, the first sample contained propane at a relatively high concentration (0.352 mg/L) compared to methane (6.26 mg/L), indicating thermogenic gas. Only trace amounts of ethane were detected in this sample. In all subsequent samples, no ethane or propane were detected. This is likely related to a sporadic pulse of thermogenic gas, especially when considering that the first sample from this well was collected after a longer purging time (90 minutes) compared to all other samples (20 minutes) except the last one, as requested by the owner. Therefore, the first sample may have caught a thermogenic gas pulse present in water from a deeper horizon. With the exception of this single sample from Zone 9R, none of the wells containing propane is located along a major fault (Figure 7). Therefore, considering the distribution of propane, faults in this area do not likely represent a preferential migration pathway for deep thermogenic gas from the Utica Shale. Instead, ethane and propane in groundwater could originate from the shallow bedrock, which does contain various levels of methane, ethane and propane (Lavoie et al., 2016).

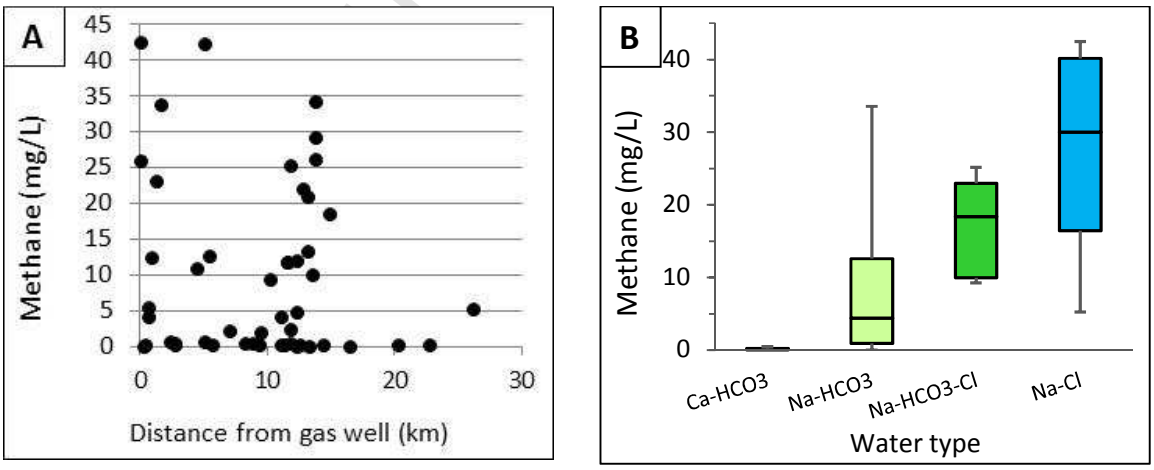

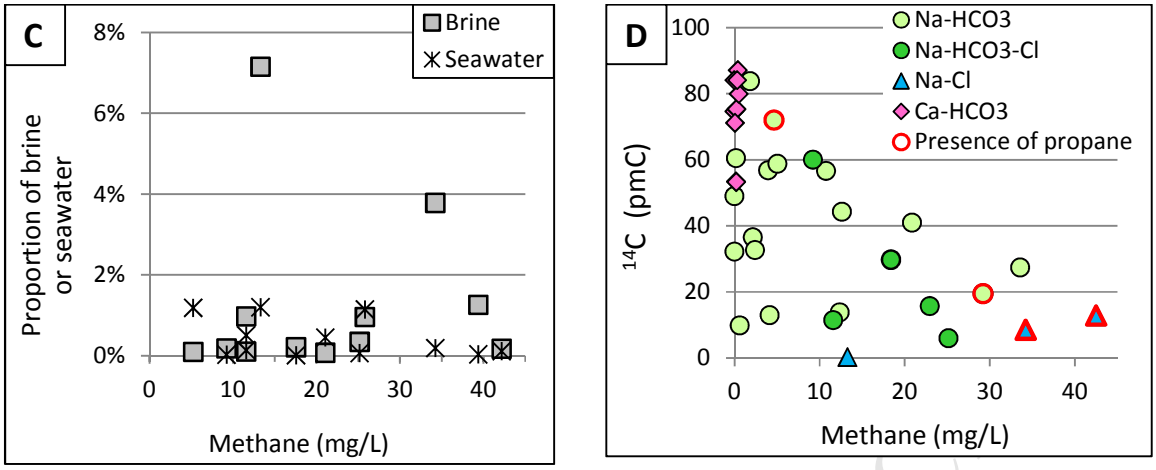

Figure 8: Concentrations of methane as related to A) distance from A267/275 gas wells, B) water type, C) proportion of brine and seawater in the sample, and D) radiocarbon values. On D, a red outline indicates presence of propane in this well, including Zone 9R where propane was only detected in 1 of 12 samples. Boxplot whiskers represent minimum and maximum values, box limits correspond to the 25th and 75th percentiles while the central line corresponds to the median value.

5.6 Conceptual hydrogeological model

Figure 9 presents the conceptual hydrogeological model that was developed for the study area using the geological and geochemical information presented in the previous sections, together with the hydrogeological conditions presented in Ladevèze et al. (2016) and Ladevèze (2017). The absence of spatial correlation along the regional groundwater flow direction concerning water types, salinity and methane, indicates that most of the groundwater flow is shallow and rather local, while deeper regional flow is limited. This has also been confirmed by modelling work (Janos, 2017). The main transitions in groundwater geochemical conditions are therefore observed vertically more than laterally (see Figure 4-A).

The shallow depth at which the little-evolved Ca-HCO_3 water type is usually found (median sampling depth of 18.3 m), the modern composition (^{14}C, tritium) of this water type, and its apparent vulnerability to surface contaminants indicate the presence of unconfined fractured intervals within the upper bedrock in which most of the active groundwater flow takes place. This is supported by the work of Ladevèze (2017), who found that most of the open fractures

are located within the upper 30 m of bedrock. Groundwater in this upper part of the fractured rock aquifer is composed of recent meteoric water dissolving carbonates as it percolates, becoming enriched in Ca^{2+} compared to freshwater from rain and snow melt. The conditions are not favorable for methanogens (presence of oxygen, positive redox values), and thus, methane concentrations are typically very low (<0.006 to 0.49 mg/L, with a median of 0.08 mg/L).

Water percolating downwards then progressively exchanges Na^{+} cations found on the clay minerals against dissolved Ca^{2+} cations, and thus evolves into Na-HCO_3-type water (median sample depth for this water type is 26.7 m), which is a transitional type that can likely be found under either unconfined, semi-confined or confined conditions. It follows that methane concentrations in this part of the aquifer are highly variable (<0.006 to 33.6 mg/L, with a median of 4.4 mg/L).

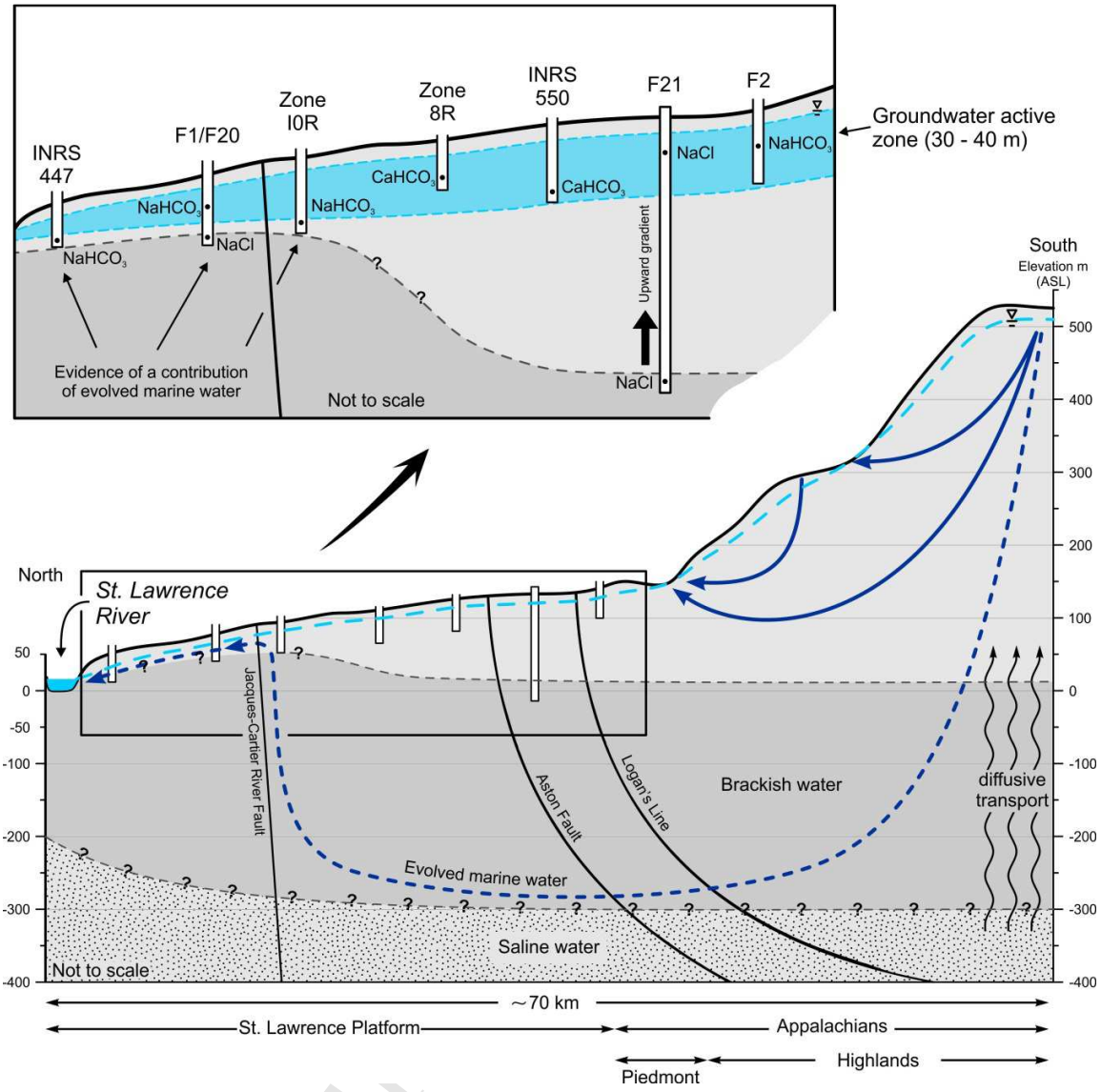

Figure 9: Conceptual groundwater flow model of the Saint-Édouard region. Actual subsurface elevations for brackish (marine) and saline (formation) waters are unknown, and should be considered best estimates with current knowledge.

Deeper in the aquifer, natural fracture density rapidly decreases, resulting in low hydraulic conductivities that greatly limit groundwater flow, with conditions being mostly confined. Evolved meteoric water, which has resided for a long time in these low-K shales, could have also mixed with residual water from the Champlain Sea, thus transitioning towards Na-HCO_3-Cl and Na-Cl types. The observed anoxic and reducing conditions are favorable to the presence of

high methane concentrations, and observed geometrically-averaged concentrations at these sampling points are between 5.3 and 42.5 mg/L.

In some areas, groundwater seems to have also been modified by the addition of limited amounts of formation brines with low Cl/Br ratio in comparison with seawater, as illustrated by the long dotted arrow in Figure 9. Such brine contribution is observed notably at well F21, which is the deepest observation well (147 m) located between the Aston Fault and the Logan's Line, next to the gas wells. In this case, it is not clear whether the brine is normally found at this depth (as there are no other wells at similar depths to corroborate results), or whether it is being transported along fractures or in carbonate slices within the thrust fault zone. In contrast, the brine contribution that was detected in shallower observation wells (≤ 50 m) located close to and downgradient from the normal Jacques-Cartier River fault, is clearly migrating upwards along this fault zone. In fact, the Jacques-Cartier River fault is likely acting both as a barrier and a conduit,with siltstone beds that could have been dragged into the gouge-sealed core, resulting in slightly more permeable zones in its upper part (Ladevèze, 2017). Following this conceptual model, the incoming relatively deep regional flow of saline or brackish groundwater coming from the Appalachians cannot cross the fault due to the low-K core filled with gouge, but instead migrate upwards through the more permeable zone upstream of it, until it reaches the active groundwater flow zone in the upper part of the bedrock aquifer.

Such cross-formational pathways allowing the migration of deeper saline fluids into fresher shallow aquifers have been observed in several other regions (e.g.: Farber et al., 2004; Hogan et al., 2007; Li et al., 2016; Warner et al., 2012; Weaver et al., 1995). A notable example is Northeastern Pennsylvania, where Warner et al. (2012) observed upward brine migration in valleys corresponding to regional groundwater discharge areas, and hypothesized that regions with a combination of natural preferential flow pathways and deep high hydrodynamic pressure, could lead to the flow of deeper fluids towards the surface. Such conditions are consistent with our study area; however in our case, the amount of brine in the samples is not correlated with methane concentrations, and therefore it appears that the brine is not a major source of methane. This result therefore suggests that major geological features in the study

area, such as the Jacques-Cartier River normal fault, may serve as preferential migration pathways for deeper fluids from the intermediate zone, and while it is unlikely to reach as deep as the Utica Shale, the actual depth of these open migration pathways is still unknown. As noted by a few authors, future research should be devoted to understanding brine migration pathways, confirm brine source, and determine the timescales for possible brine migration, in order to assess whether the pathways could represent a risk for aquifer contamination in the context of hydraulic fracturing (Vidic et al., 2013; Warner et al., 2012).

6 Conclusions

In this study, we investigated the natural baseline hydrogeochemistry of the rural region of Saint-Édouard (St. Lawrence Lowlands, eastern Canada), a region where dissolved methane is ubiquitous in aquifers and where only two exploration gas wells (one vertical and one horizontal) were drilled into the Utica Shale in 2009. The horizontal well was hydraulically fractured at the beginning of 2010. The distribution of dissolved alkanes (methane, ethane, propane) in these shallow aquifers, mainly composed of organic-rich black shale, was interpreted in terms of underlying geology, hydrogeology and groundwater chemistry. Methane concentrations vary widely over very short distances and were found to be mainly correlated to water type, aquifer confinement conditions and bedrock geology (black shale-dominated versus succession composed of alternating shale and siltstone, dolomite and/or limestone). The highest methane concentrations were generally found below the active groundwater flow zone, where bedrock aquifer conditions become semi-confined to confined due to either low-permeability surficial sediments, or poorly fractured bedrock intervals above flowing fractures.

Two distinct sources of salinity were identified in shallow wells, namely residual seawater from the Champlain Sea and formation brines flowing upwards. The presence of brine was especially noticeable along the Jacques-Cartier River fault, indicating connectivity between the shallow aquifer and somewhat deeper strata. Such connectivity was suggested by Pinti et al. (2013) for the Yamaska Fault, which is a southeast extension of the Jacques-Cartier River fault, due to the higher methane concentrations they had observed along this fault and other regional faults. In

our study, however, the normal fault is not associated with higher methane concentrations, and in most (but not all) sampled locations near the fault, the gas appears to be of microbial origin, as shown by the absence of ethane and propane. At the moment, there is no indication that the connectivity would extend as deep as the Utica Shale, which is located at depths of approximately 500 m near this fault. However, the targeted development zone in this region is located to the south, near the Appalachian domain where the gas-rich shales are deeper (2000 m). All exploration wells (conventional and unconventional) with publicly available pressure data in southern Quebec have shown overpressure conditions in the Utica Shale, thus suggesting no communication with the surface (Aguilera, 1978; Chatellier et al., 2013). Further work would be highly recommended in order to assess the depth from which the brine originates. If shale gas development activities were to resume, it would be important to determine whether this fault, in this region and along its western extension, could serve as a preferential pathway for gas, brine and drilling/fracturing fluids injected at high pressures in the Utica Shale. This would also need to be done for any other deep industrial activities, including brine exploitation, injection of CO_2 and underground gas storage.

More generally, this is one of the first multi-approach baseline studies of a groundwater system in an area with significant potential of hydrocarbon development, before any large-scale drilling and fracturing operations have taken place. As such, it sheds light on factors that may control the distribution of methane in shallow groundwater and on the possibility of upward migration from deeper horizons under pristine natural conditions. Several observations made in this study may be applicable to other regions when formulating working hypotheses for new baseline studies. This study also demonstrated that different scales may prove enlightening to better understand the hydrogeological system. On the one hand, the high methane variability that was observed over very short distances highlights the need to sample a large number of private wells within a reasonable distance from a planned shale gas well, and not only for alkanes, but also for general chemistry parameters in order to have a good understanding of each well's behavior. Having a dense sampling network is crucial to address industry liability issues, especially for contamination that could arise from handling and storage activities, or contaminant migration along faulty casings. On the other hand, the presence of formation

brines in the shallow aquifer along the Jacques-Cartier River fault demonstrates that regional or semi-regional studies with lower sample density are also necessary in order to understand the hydrodynamics of the regional system and, therefore, identify geological features that could potentially serve as migration pathways for deep fluids. Such pathways could possibly facilitate the migration of deep fluids over lateral distances from a shale gas well much greater than those expected for contamination related to surface activities or faulty casings.

7 Acknowledgements

The authors would first like to thank the residents of the Saint-Édouard area who provided access to their water well, or who allowed us to drill observation wells on their land. Without their much appreciated collaboration, this project could not have been carried out. We are also grateful to Dr. Jason Ahad (internal reviewer) and to the anonymous journal reviewers for their thorough review and valuable suggestions. Our gratitude is extended to all technical staff from the GSC-Quebec Delta-Lab, the INRS general laboratory, the University of Ottawa G.G. Hatch laboratory, and the Environmental Isotope Laboratory of the University of Waterloo. A special thanks goes to Susan Zimmerman from the Lawrence Livermore National Laboratory for her great help with chlorine 36 analyses, and to the field crews of the Geological Survey of Canada that were involved in acquiring the data. Mrs. Marianne Molgat is thanked for her incredible support, interest and for the sharing of information and data from Talisman Energy. The project was supported by the Ministère du Développement durable, de l'Environnement et de la Lutte aux Changements climatiques du Québec (MDDELCC) in particular, Mr. Charles Lamontagne was instrumental from the start of the project. This study was funded through the ecoEnergy Innovation Initiative (ecoEII) and the Program for Energy Research and Development (PERD) of the Energy Sector (project UOSG005) and through regular funds of the Environmental Geoscience Program of the Earth Science Sector, both of Natural Resources Canada. This is Earth Science Sector contribution 20160356.

8 References

Aguilera, R., 1978. Log Analysis of Gas Bearing Fracture Shales in the Saint Lawrence Lowlands of Quebec. SPE Annual Fall Technical Conference, Houston, Texas. 1-3 October 1978. SPE 7445-MS.

Allison, M. L., 2001. Hutchinson, Kansas: A geologic detective story. Geotimes October 2001 issue.

Bair, E. S., D.C. Freeman, and J.M. Senko., 2010. Subsurface Gas Invasion, Bainbridge Township, Geauga County, Ohio. Expert Panel Technical Report submitted to Ohio Dept. of Natural Resources.

Benoit, N., Nastev, M., Blanchette, D. and Molson, J., 2014. Hydrogeology and hydrogeochemistry of the Chaudière River watershed aquifers, Québec, Canada. Canadian Water Resources Journal 39(1): 32-48.

Bentley, H.W., Phillips, F.M., Davis, S.N. 1986. Chlorine-36 in the terrestrial environment. Chapter 10, *In: P. Fritz and J.-Ch. Fontes, (Eds.) Handbook of Environmental Isotope Geochemistry, Vol. 2, The Terrestrial Environment, B.* Elsevier, Amsterdam, The Netherlands: 427-480.

Boyer, E. W., Swistock, B. R., Clark, J., Madden, M. and Rizzo, D. E., 2012. The impact of Marcellus gas drilling on rural drinking water supplies. The Center for Rural Pennsylvania, Pennsylvania General Assembly, Harrisburg, PA, 26 p.

Castonguay, S., Dietrich, J., Lavoie, D. and Laliberté, J. Y., 2010. Structure and petroleum plays of the St. Lawrence Platform and Appalachians in southern Quebec: Insights from interpretation of MRNQ seismic reflection data. Bulletin of Canadian Petroleum Geology 58(3): 219-234.

CCA, 2014. Environmental impacts of shale gas extraction in Canada. The expert panel on harnessing science and technology to understand the environmental impacts of shale gas extraction, Council of Canadian Academies, 262 p.

Chatellier, J. Y., Flek, P., Molgat, M., Anderson, I., Ferworn, K., Larsen, N. L. and Ko, S., 2013. Overpressure in shale gas: When geochemistry and reservoir engineering data meet and agree. AAPG Memoir 103, p. 45-69.

Chen, Z., Lavoie, D. and Malo, M., 2014. Geological Characteristics and Petroleum Resource Assessment of Utica Shale, Quebec, Canada. Geological Survey of Canada, Open File 7606, 43 p.

Clark, I. and Fritz, P., 1997. Environmental Isotopes in Hydrogeology. CRC Press, Boca Raton, FL, 328 p.

Clark, T. H. and Globensky, Y., 1973. Portneuf et parties de Saint-Raymond et de Lyster - Comtés de Portneuf et de Lotbinière. Ministère des Richesses Naturelles - Direction Générale des Mines, Rapport Géologique RG-148, 110 p.

Cloutier, V., Lefebvre, R., Therrien, R. and Savard, M., 2008. Multivariate statistical analysis of geochemical data as indicative of the hydrogeochemical evolution of groundwater in a sedimentary rock aquifer system. Journal of Hydrology 353(3-4): 294-313.

Cloutier, V., Lefebvre, R., Savard, M. M. and Therrien, R., 2010. Desalination of a sedimentary rock aquifer system invaded by Pleistocene Champlain Sea water and processes controlling groundwater geochemistry. Environmental Earth Sciences 59(5): 977-994.

Comeau, F. A., Kirkwood, D., Malo, M., Asselin, E. and Bertrand, R., 2004. Taconian mélanges in the parautochthonous zone of the Quebec Applachians revisited: Implications for foreland basin and thrust belt evolution. Canadian Journal of Earth Sciences 41(12): 1473-1490.

Considine, T., Watson, R., Considine, N. and Martin, J., 2012. Environmental impacts during Marcellus Shale gas drilling: causes, impacts, and remedies. Shale Resources And Society Institute, University at Buffalo—The State University of New York, Report 2012–1, 52 p.

Craig, H., 1961. Isotopic variations in meteoric waters. Science 133: 1702-1703.

Crow, H. L. and Ladevèze, P., 2015. Downhole geophysical data collected in 11 boreholes near St-Édouard-de-Lotbinière, Québec. Geological Survey of Canada, Open file 7768, 48 p.

Darrah, T. H., Vengosh, A., Jackson, R. B., Warner, N. R. and Poreda, R. J., 2014. Noble gases identify the mechanisms of fugitive gas contamination in drinking-water wells overlying the Marcellus and Barnett Shales. Proceedings of the National Academy of Sciences of the United States of America 111(39): 14076-14081.

Davies, R. J., 2011. Methane contamination of drinking water caused by hydraulic fracturing remains unproven. Proceedings of the National Academy of Sciences of the United States of America 108(43): E871.

Davis, J. B. and Squires, R. M., 1954. Detection of microbially produced gaseous hydrocarbons other than methane. Science 119: 381.

Davis, S. N., Fabryka-Martin, J., Wolfsberg, L., Moysey, S., Shaver, R., Calvin Alexander Jr, E. and Krothe, N., 2000. Chlorine-36 in ground water containing low chloride concentrations. Ground Water 38(6): 912-921.

Dusseault, M. and Jackson, R., 2014. Seepage pathway assessment for natural gas to shallow groundwater during well stimulation, in production, and after abandonment. Environmental Geosciences 21(3): 107-126.

Engelder, T., 2012. Capillary tension and imbibition sequester frack fluid in Marcellus gas shale. Proceedings of the National Academy of Sciences of the United States of America 109(52): E3625.

EPA, 2012. Study of the potential impacts of hydraulic fracturing on drinking water resources. United States Environmental Protection Agency (US EPA), Office of research and development, Progress report EPA 601/R-12/011, 278 p.

Farber, E., Vengosh, A., Gavrieli, I., Marie, A., Bullen, T. D., Mayer, B., Holtzman, R., Segal, M. and Shavit, U., 2004. The origin and mechanisms of salinization of the Lower Jordan River. Geochimica et Cosmochimica Acta 68(9): 1989-2006.

Flewelling, S. A. and Sharma, M., 2015. Comment on ‘‘Hydraulic fracturing in faulted sedimentary basins: Numerical simulation of potential contamination of shallow aquifers over long time scales’’ by C. Gassiat et al. Water Resources Research 51(3): 1872-1876.

Gassiat, C., Gleeson, T., Lefebvre, R. and McKenzie, J., 2013. Hydraulic fracturing in faulted sedimentary basins: numerical simulation of potential contamination of shallow aquifers over long time scales. Water Resources Research 49(12): 8310-8327.

Globensky, Y., 1987. Géologie des Basses-Terres du Saint-Laurent, Québec. Ministère des Richesses naturelles, Québec, MM Report 85-02, 63 p.

Hamblin, A. P., 2006. The "shale gas" concept in Canada: a preliminary inventory of possibilities. Geological Survey of Canada, Open File 5384, 108 p.

Hillaire-Marcel, C., 1977. Les isotopes du carbone et de l’oxygène dans les mers post-glaciaires du Québec. Géographie physique et Quaternaire 31(1-2): 81-106.

Hillaire-Marcel, C., 1988. Isotopic composition (18O, 13C, 14C) of biogenic carbonates in Champlain Sea Sediments. In: The late Quaternary Development of the Champlain Sea Basin. Geological Association of Canada, Special Paper 35, p. 177-194.

Hogan, J. F., Phillips, F. M., Mills, S. K., Hendrickx, J. M. H., Ruiz, J., Chesley, J. T. and Asmerom, Y., 2007. Geologic origins of salinization in a semi-arid river: The role of sedimentary basin brines. Geology 35(12): 1063-1066.

Hounslow, A. W., 1995. Water Quality Data Analysis and Interpretation. Lewis Publishers, Boca Raton, FL, 379 p.

Humez, P., Mayer, B., Ing, J., Nightingale, M., Becker, V., Kingston, A., Akbilgic, O. and Taylor, S., 2016a. Occurrence and origin of methane in groundwater in Alberta (Canada): Gas geochemical and isotopic approaches. Science of the Total Environment 541: 1253-1268.

Humez, P., Mayer, B., Nightingale, M., Becker, V., Kingston, A., Taylor, S., Bayegnak, G., Millot, R. and Kloppman, W., 2016b. Redox controls on methane formation, migration and fate in shallow aquifers. Hydrology and Earth System Sciences 20: 2759-2777.

Jackson, R. B., Osborn, S. G., Vengosh, A. and Warner, N. R., 2011. Reply to Davies: Hydraulic fracturing remains a possible mechanism for observed methane contamination of drinking water. Proceedings of the National Academy of Sciences of the United States of America 108(43).

Jackson, R. B., Vengosh, A., Darrah, T. H., Warner, N. R., Down, A., Poreda, R. J., Osborn, S. G., Zhao, K. and Karr, J. D., 2013a. Increased stray gas abundance in a subset of drinking water wells near Marcellus shale gas extraction. Proceedings of the National Academy of Sciences of the United States of America 110(28): 11250-11255.

Jackson, R. E., Gorody, A. W., Mayer, B., Roy, J. W., Ryan, M. C. and Van Stempvoort, D. R., 2013b. Groundwater protection and unconventional gas extraction: The critical need for field-based hydrogeological research. GroundWater 51(4): 488-510.

Janos, D., 2017. Regional Groundwater Flow Dynamics and Residence Times in Chaudière-Appalaches, Québec, Canada: Insights from Numerical Simulations. M.Sc. thesis, Laval University.

Jarvie, D. M., 2012a. Shale resource systems for oil and gas: Part 1—Shale-gas resource systems, In: J. A. Breyer, ed., Shale reservoirs—Giant resources for the 21st century. AAPG, Memoir 97, p. 69–87.

Jarvie, D. M., 2012b. Shale resource systems for oil and gas: Part 2—Shale-oil resource systems. In: J. A. Breyer, ed., Shale reservoirs—Giant resources for the 21st century. AAPG, Memoir 97, p. 89–119.

Kampbell, D. H. and Vandegrift, S. A., 1998. Analysis of Dissolved Methane, Ethane, and Ethylene in Ground Water by a Standard Gas Chromatographic Technique. Journal of Chromatographic Science 36(5): 253-256.

Kappell, W. M. and Nystrom, E. A., 2012. Dissolved Methane in New York Groundwater. United States Geological Survey, Open-file Report 2012-1162, 6 p.

Katz, B.G., Eberts, S.M., Kauffman, L.J., 2011. Using Cl/Br ratios and other indicators to assess potential impacts on groundwater quality from septic systems: A review and examples from principal aquifers in the United States. Journal of Hydrology 397: 151-166.

Kennedy, G. W. and Drage, J., 2015. Assessing patterns of dissolved methane in shallow aquifers related to Carboniferous and Triassic sedimentary basins, Nova Scotia, Canada. Atlantic Geology 51: 233-241.

Kissinger, A., Helmig, R., Ebigbo, A., Class, H., Lange, T., Sauter, M., Heitfeld, M., Klünker, J. and Jahnke, W., 2013. Hydraulic fracturing in unconventional gas reservoirs: Risks in the geological system, part 2: Modelling the transport of fracturing fluids, brine and methane. Environmental Earth Sciences 70(8): 3855-3873.

Konstantinovskaya, E. A., Rodriguez, D., Kirkwood, D., Harris, L. B. and Thériault, R., 2009. Effects of basement structure, sedimentation and erosion on thrust wedge geometry: an example from the Quebec Appalachians and Analogue models. Bulletin of Canadian Petroleum Geology 57: 34-62.

Ladevèze, P., Rivard, C., Lefebvre, R., Lavoie, D., Parent, M., Malet, X., Bordeleau, G. and Gosselin, J., 2016. Travaux de caractérisation hydrogéologique dans la plateforme sédimentaire du Saint-Laurent, région de Saint-Édouard-de-Lotbinière, Québec. Geological Survey of Canada, Open file 8036, 112 p.

Ladevèze, P., 2017. Aquifères superficiels et ressources profondes: le rôle des failles et des réseaux de fractures, Ph.D. thesis, INRS-ETE, 117 pages.

Lavoie, D., 2008. Appalachian Foreland Basin of Canada. Sedimentary Basins of the World 5: 65-103.

Lavoie, D., Rivard, C., Lefebvre, R., Séjourné, S., Thériault, R., Duchesne, M. J., Ahad, J. M. E., Wang, B., Benoit, N. and Lamontagne, C., 2014. The Utica Shale and gas play in southern Quebec: Geological and hydrogeological syntheses and methodological approaches to groundwater risk evaluation. International Journal of Coal Geology 126: 77-91.

Lavoie, D., Pinet, N., Bordeleau, G., Ardakani, O. H., Ladevèze, P., Duchesne, M. J., Rivard, C., Mort, A., Brake, V., Sanei, H. and Malet, X., 2016. The Upper Ordovician black shales of southern Quebec (Canada) and their significance for naturally occurring hydrocarbons in shallow groundwater. International Journal of Coal Geology 158: 44-64.

Lefebvre, R., Ballard, J. M., Carrier, M. A., Vigneault, H., Beaudry, C., Berthot, L., Légaré-Couture, G., Parent, M., Laurencelle, M., Malet, X., Therrien, A., Michaud, A., Desjardins, J., Drouin, A., Cloutier, M. H., Grenier, J., Bourgault, M. A., Larocque, M., Pellerin, S., Graveline, M. H., Janos, D. and Molson, J., 2015. Portrait des ressources en eau souterraine en Chaudière-Appalaches, Québec, Canada. Final Report INRS R-1580 prepared for the MDDELCC, 246 p.

Lefebvre, R., 2017. Mechanisms leading to potential impacts of shale gas development on groundwater quality. WIREs Water 4(1): 15 p.

Li, Z., You, C., Gonzales, M., Wendt, A. K., Wua, F. and Brantley, S. L., 2016. Searching for anomalous methane in shallow groundwater near shale gas wells. Journal of Contaminant Hydrology 195: 23-30.

Loomer, D. B., MacQuarrie, K. T. B., Bragdon, I. K., Connor, D. A., Loomer, H. A., Leblanc, J. F. and Nason, B., 2016. Baseline Assessment of Private Well Water Quality in Areas of Potential Shale Gas Development in New Brunswick. Final Report prepared for the New Brunswick Energy Institute Fredericton, NB, 216 p.

Martini, A. M., Walter, L. M., Budat, J. M., Ku, T. C. W., Kaiser, C. J. and Schoell, M., 1998. Genetic and temporal relations between formation waters and biogenic methane: Upper Devonian Antrim shale, Michigan Basin, USA. Geochimica et Cosmochimica Acta 62(10): 1699-1720.

McIntosh, J. C., Grasby, S. E., Hamilton, S. M. and Osborn, S. G., 2014. Origin, distribution and hydrogeochemical controls on methane occurrences in shallow aquifers, southwestern Ontario, Canada. Applied Geochemistry 50: 37-52.

McPhillips, L. E., Creamer, A. E., Rahm, B. G. and Walter, M. T., 2014. Assessing dissolved methane patterns in central New York groundwater. Journal of Hydrology: Regional Studies 1: 57-73.

MDDELCC (Ministère du Développement durable, de l'Environnement et de la Lutte contre les Changements climatiques). 2017. Règlement sur le prélèvement des eaux et leur protection, Loi sur la qualité de l'environnement, Chapitre V: Site de forage destiné à rechercher ou à exploiter du pétrole, du gaz naturel, de la saumure ou un réservoir souterrain, http://legisquebec.gouv.qc.ca/fr/ShowDoc/cr/Q-2,%20r.%2035.2.

Molofsky, L. J., Connor, J. A., Farhat, S. K., Wylie Jr, A. S. and Wagner, T., 2011. Methane in Pennsylvania water wells unrelated to Marcellus shale fracturing. Oil and Gas Journal 109(19): 54-67+93.

Molofsky, L. J., Connor, J. A., Wylie, A. S., Wagner, T. and Farhat, S. K., 2013. Evaluation of Methane Sources in Groundwater in Northeastern Pennsylvania. GroundWater 51(3): 333-349.

Molofsky, L. J., Connor, J. A., McHugh, T. E., Richardson, S. D., Woroszylo, C. and Alvarez, P. J., 2016. Environmental Factors Associated With Natural Methane Occurrence in the Appalachian Basin. GroundWater 54(5): 656-668.

Moritz, A., Hélie, J. F., Pinti, D. L., Larocque, M., Barnetche, D., Retailleau, S., Lefebvre, R. and Gélinas, Y., 2015. Methane baseline concentrations and sources in shallow aquifers from the shale gas-prone region of the St. Lawrence lowlands (Quebec, Canada). Environmental Science and Technology 49(7): 4765-4771.

Nowamooz, A., Lemieux, J. M., Molson, J. and Therrien, R., 2015. Numerical investigation of methane and formation fluid leakage along the casing of a decommissioned shale gas well. Water Resources Research 51(6): 4592-4622.

Occhietti, S., 2007. The Saint-Narcisse morainic complex and early Younger Dryas events on the southeastern margin of the Laurentide Ice Sheet. Géographie physique et Quaternaire 61(2-3): 89-118.

Osborn, S. G., Vengosh, A., Warner, N. R. and Jackson, R. B., 2011. Methane contamination of drinking water accompanying gas-well drilling and hydraulic fracturing. Proceedings of the National Academy of Sciences of the United States of America 108(20): 8172-8176.

PA-DEP, 2012. Light Hydrocarbons in Aqueous Samples via Headspace and Gas Chromatography with Flame Ionization Detection (GC/FID), Rev. 1. Pennsylvania Department of Environmental Protection, Method 3686, 13 p.

Pinti, D. L., Gélinas, Y., Larocque, M., Barnetche, D., Retailleau, S., Moritz, A., Hélie, J. and Lefebvre, R., 2013. Concentrations, sources et mécanismes de migration préférentielle des gaz d'origine naturelle (méthane, hélium, radon) dans les eaux souterraines des Basses-

Terres du Saint-Laurent. Volet Géochimie. UQAM, U. Concordia, INRS-ETE, Étude E3-9, FQRNT ISI n° 171083, 94 p.

Reagan, M. T., Moridis, G. J., Keen, N. D. and Jonhson, J. N., 2015. Numerical simulation of the environmental impact of hydraulic fracturing of tight/shale gas reservoirs on near-surface groundwater: Background, base cases, shallow reservoirs, short-term gas, and water transport. Water Resources Research 51(4): 2543-2573.

Révész, K. M., Breen, K. J., Baldassare, A. J. and Burruss, R. C., 2010. Carbon and hydrogen isotopic evidence for the origin of combustible gases in water-supply wells in north-central Pennsylvania. Applied Geochemistry 25(12): 1845-1859.

Rivard, C., Lavoie, D., Lefebvre, R., Séjourné, S., Lamontagne, C. and Duchesne, M., 2014. An overview of Canadian shale gas production and environmental concerns. International Journal of Coal Geology 126: 64-76.

Rivard, C., Bordeleau, G., Lavoie, D., Lefebvre, R. and Malet, X., 2017a. Temporal variations of methane concentration and isotopic composition in groundwater of the St. Lawrence Lowlands, eastern Canada. Hydrogeology Journal, https://doi.org/10.1007/s10040-017-1677-y.

Rivard, C., Bordeleau, G., Lavoie, D., Lefebvre, R. and Malet, X., 2017b. Can groundwater sampling techniques used in monitoring wells influence methane concentrations and isotopes? Environmental Monitoring and Assessment (accepted).

Saba, T. and Orzechowski, M., 2011. Lack of data to support a relationship between methane contamination of drinking water wells and hydraulic fracturing. Proceedings of the National Academy of Sciences of the United States of America 108(37).

Schon, S. C., 2011. Hydraulic fracturing not responsible for methane migration. Proceedings of the National Academy of Sciences of the United States of America 108(37).

Séjourné, S., Lefebvre, R., Malet, X. and Lavoie, D., 2013. Synthèse géologique et hydrogéologique du Shale d'Utica et des unités sus-jacentes (Lorraine, Queenston et dépôts meubles), Basses-Terres du Saint-Laurent, Province de Québec. Geological Survey of Canada, Open file 7338, 165 p.

Sharma, S. and Baggett, J. K., 2011. Application of carbon isotopes to detect seepage out of coalbed natural gas produced water impoundments. Applied Geochemistry 26(8): 1423-1432.

Shields, G. A., Carden, G. A. F., Veizer, J., Meidla, T., Rong, J. Y. and Li, R. Y., 2003. Sr, C, and O isotope geochemistry of Ordovician brachiopods: A major isotopic event around the Middle-Late Ordovician transition. Geochimica et Cosmochimica Acta 67(11): 2005-2025.

Siegel, D., Smith, B., Perry, E., Bothun, R. and Hollingsworth, M., 2016. Dissolved methane in shallow groundwater of the Appalachian Basin: Results from the Chesapeake Energy predrilling geochemical database. Environmental Geosciences 23(1): 1-47.

Siegel, D. I., Azzolina, N. A., Smith, B. J., Perry, A. E. and Bothun, R. L., 2015a. Methane concentrations in water wells unrelated to proximity to existing oil and gas wells in northeastern Pennsylvania. Environmental Science and Technology 49(7): 4106-4112.

Siegel, D. I., Smith, B., Perry, E., Bothun, R. and Hollingsworth, M., 2015b. Pre-drilling water-quality data of groundwater prior to shale gas drilling in the Appalachian Basin: Analysis of the Chesapeake Energy Corporation dataset. Applied Geochemistry 63: 37-57.

SIGPEG, 2017. Oil and gas geoscience information system - Well data. http://sigpeg.mrn.gouv.qc.ca/gpg/classes/rechercheIGPG. Accessed January 2017.

Tremblay, A. and Pinet, N., 2016. Late Neoproterozoic to Permian tectonic evolution of the Quebec Appalachians, Canada. Earth-Science Reviews 160: 131-170.

Vengosh, A., Jackson, R. B., Warner, N., Darrah, T. H. and Kondash, A., 2014. A critical review of the risks to water resources from unconventional shale gas development and hydraulic fracturing in the United States. Environmental Science and Technology 48(15): 8334-8348.

Vidic, R. D., Brantley, S. L., Vandenbossche, J. M., Yoxtheimer, D. and Abad, J. D., 2013. Impact of shale gas development on regional water quality. Science 340(6134): 1235009.

Vogel, T. M., Oremland, R. S. and Kvenvolden, K. A., 1982. Low-temperature formation of hydrocarbon gases in San Francisco Bay sediment (California, U.S.A.). Chemical Geology 37: 289-298.

Warner, N. R., Jackson, R. B., Darrah, T. H., Osborn, S. G., Down, A., Zhao, K., White, A. and Vengosh, A., 2012. Geochemical evidence for possible natural migration of Marcellus Formation brine to shallow aquifers in Pennsylvania. Proceedings of the National Academy of Sciences of the United States of America 109(30): 11961-11966.

Weaver, T. R., Frape, S. K. and Cherry, J. A., 1995. Recent cross-formational fluid flow and mixing in the shallow Michigan Basin. Bulletin of the Geological Society of America 107(6): 697-707.

Whiticar, M. J., Faber, E. and Schoell, M., 1986. Biogenic methane formation in marine and freshwater environments: CO_2 reduction vs. acetate fermentation - isotope evidence. Geochimica et Cosmochimica Acta 50: 693-709.

9 Supplementary Information

9.1 ^{36}Cl calculations

In this section, the term $R^{36}Cl$ will be used as a shorter term to refer to the $^{36}Cl/Cl$ ratio multiplied by 10^{15} (see section 4.4 of the manuscript for details). The age of the chlorine in groundwater may be computed from the $R^{36}Cl$ in a sample at time *t* (R_t), assuming one knows the initial ratio (R_0) at the time of recharge. This initial ratio is the result of cosmogenic sources of ^{36}Cl (bombardment of ^{40}Ar, ^{36}Ar and ^{35}Cl in the upper stratosphere), and epigenic sources (activation and spallation of Cl, K, Ca and Ar by cosmic radiation penetrating the near-surface rocks and soils; Clark and Fritz, 1997). Such ratios for different geographic locations in North America have been mapped by Davis et al. (2000). Based on this map, R_0 for our study area should be between 400 and 800. Decay of R_0 over time may be calculated using the ^{36}Cl half-life of 301 000 years (see Eq. S1 below).

Hypogenic ^{36}Cl buildup (Eq. S2) must also be considered, which is the result of ^{35}Cl being acted upon by naturally produced thermal neutrons at all depths in the subsurface. With time, hypogenic ^{36}Cl will accumulate and decay until the rate of production and decay are similar, i.e. secular equilibrium is reached. This usually occurs after about 5 half-lives, or 1.5 million years (Clark and Fritz, 1997). Hypogenic ^{36}Cl production depends on the neutron flux and varies between geological settings; secular equilibrium ratios (R_{se}) were computed by Bentley et al. (1986) for different environmental settings. The values retained for our study area are those of shales (R_{se}= 12.5) and sandstones (R_{se}= 4.68), as the local lithologies are composed mainly of shales with interbeds of siltstones (Lavoie et al., 2016).

Decay of cosmogenic + epigenic ^{36}Cl in recharge water over time: $\boldsymbol{R_t = R_0 exp(-\lambda t)}$ **Eq. S1**

Hypogenic production of ^{36}Cl: $\boldsymbol{R_t = R_{se}\,[1 - \exp(-\lambda t)]}$ **Eq. S2**

Total $R^{36}Cl$: $\boldsymbol{R_t = R_0 \exp(-\lambda t) + R_{se}[1 - \exp(-\lambda t)]}$ **Eq. S3**

For the study area, the evolution of $R^{36}Cl$ over time may be calculated by adding the cosmogenic, epigenic and hypogenic sources (Eq. S3). Figure S-1 shows the curves for: 1) the decay of cosmogenic + epigenic ^{36}Cl (orange dashed and solid lines representing R_0 values of 400 and 800, respectively), 2) hypogenic production (green dashed and solid lines computed from secular equilibrium values for sandstones and shales, respectively), and 3) total ^{36}Cl (black dashed and solid lines representing minimum and maximum computed values).

The two groundwater samples analyzed for ^{36}Cl (F7deep, $R^{36}Cl$= 9.25 and F20deep, $R^{36}Cl$= 11.07) were also placed on the graph. Their age (1.81 million years for F7deep, 1.73 million years for F20deep) was calculated based solely on decay of cosmogenic + epigenic ^{36}Cl (Eq. S1), with an assumed mean R_0 value of 600. However, it is apparent that their measured $R^{36}Cl$ could also correspond to secular equilibrium for hypogenic production in a mixture of shales (R_{se}= 12.5) and sandstones (R_{se}= 4.68). Unfortunately, the secular equilibrium ratio for this specific region was not evaluated, and interpretation must rely on R_{se} values published in the literature. Nonetheless, it is clear that the calculated ages for the groundwater samples represent a minimum, and they could be much older if secular equilibrium has effectively been reached.

It is noteworthy that the calculated ^{36}Cl ages are related to the source of salinity in the samples, and may not necessarily represent the "true" age of the water itself. Indeed, a more modern water component may also be present, but its effect on ^{36}Cl results could be largely masked by the presence of the extremely old, saline brine that makes up most of the salinity in the samples. In the case of sample F20deep, a more recent water component is confirmed by the presence of tritium (3.6 TU) and ^{14}C-DIC (8.17 pmC). In sample F7deep, tritium and ^{14}C-DIC were undetected.

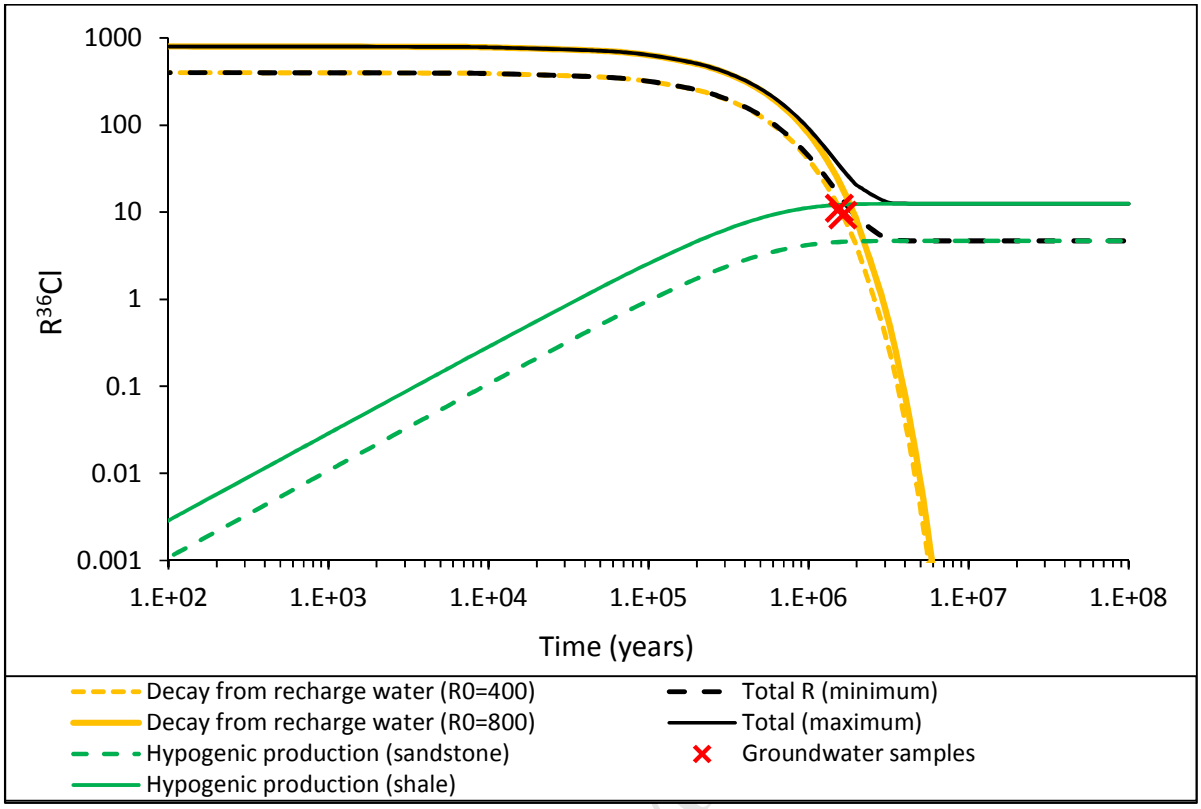

Figure S-1. Theoretical evolution of $R^{36}Cl$ ($R^{36}Cl = {}^{36}Cl/Cl \times 10^{15}$) in the local aquifer over time, and values for the two groundwater samples (F7deep and F20deep).

9.2 Other supplementary tables and figures

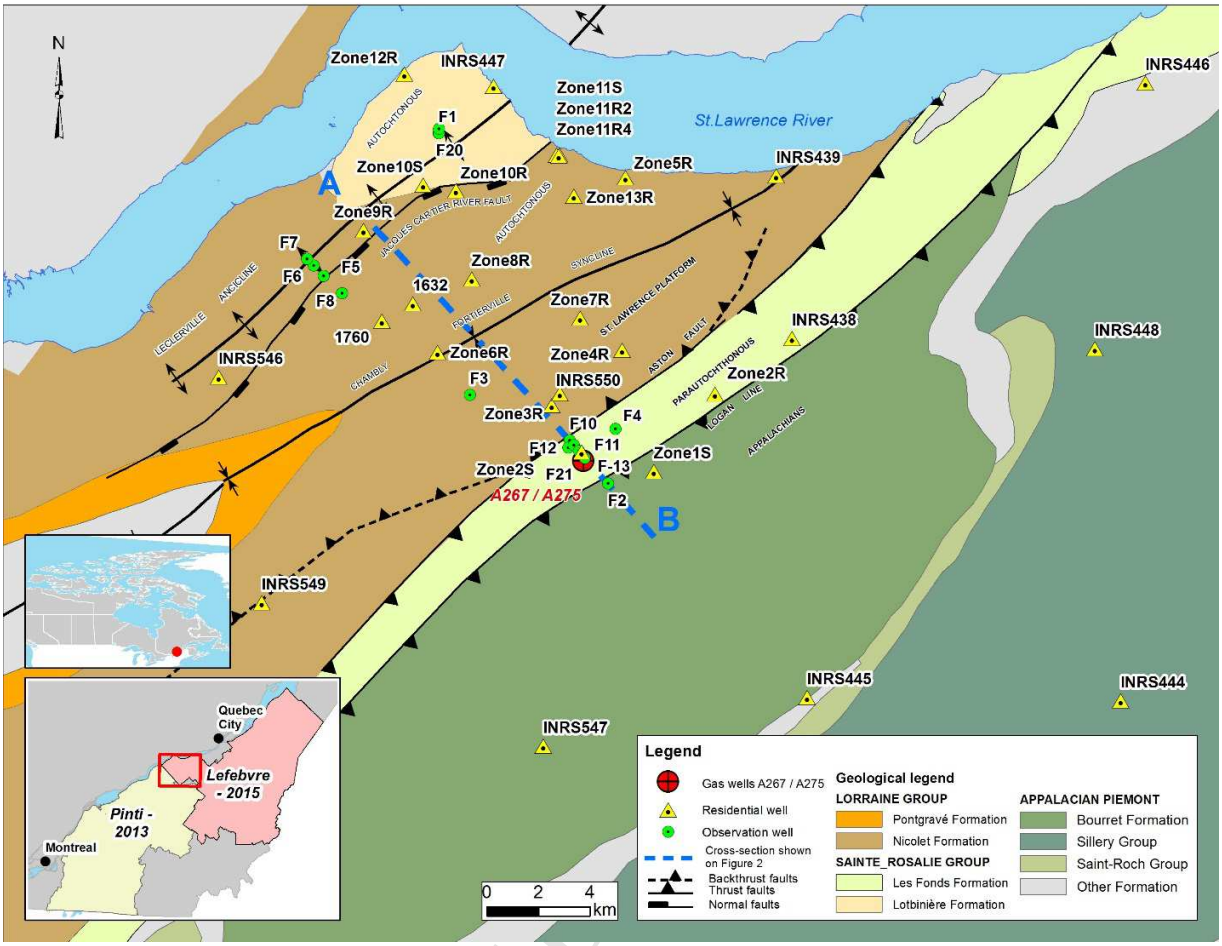

Figure S-2. Extended study area, which includes all the wells borrowed from the Lefebvre et al. (2015) study for the geochemical interpretation, some of which fall slightly outside of the 500-km^2 Saint-Édouard study area. The dotted line represents the cross-section shown on Figure 2.

Table S-1. Residential wells

Well name	Well type	Well depth (m)	Casing above ground (m)	Static water level (m TOC)	Thickness of unconsolidated sediments (m)
Zone 1S	Unconsolidated	18.3	0.65	4.34	na
Zone 2S	Unconsolidated	7.5	0.80	1.34	na
Zone 10S	Unconsolidated	4.7	0.76	0.48	na
Zone 11S	Unconsolidated	4.7	1.04	1.37	na
Zone 2R	Open bedrock	13.7	0.50	2.35	na
Zone 3R	Open bedrock	61.0	na	na	na
Zone 4R	Open bedrock	36.3	0.33	6.32	3.8
Zone 5R	Open bedrock	61.0	0.57	15.53	3.66
Zone 6R	Open bedrock	27.4	0	3.04	18.9
Zone 7R	Open bedrock	85.6	0.33	2.05	3.6
Zone 8R	Open bedrock	18.0	0.4	na	na
Zone 9R	Open bedrock	45.7	2.27	na	5.5
Zone 10R	Open bedrock	56.4	0	na	na
Zone 11R2	Open bedrock	97.6	0.5	34.12	1.2
Zone 11R4	Open bedrock	between 45 and	na	na	na
Zone 12R	Open bedrock	101.2	na	82.32	<4
Zone 13R	Open bedrock	50.0	0.52	3.28	0.85
1632	Open bedrock	83.8	na	na	na
1760	Open bedrock	50.3	na	na	na
INRS-438	Open bedrock	88.4	na	na	na
INRS-439	Open bedrock	91.4	na	na	na
INRS-444	Open bedrock	32.0	na	na	na
INRS-445	Open bedrock	18.3	na	na	na
INRS-446	Open bedrock	25.9	na	na	na
INRS-447	Open bedrock	12.8	na	na	na
INRS-448	Open bedrock	52.4	na	na	na
INRS-546	Open bedrock	21.9	na	na	na
INRS-547	Open bedrock	33.5	na	na	na
INRS-550	Open bedrock	51.2	na	na	na
INRS-549	Open bedrock	45.7	na	na	na

na: not available

m TOC: meters from top of casing

Table S-2. Observation wells

Well name	Drilling date	Total well depth (m)	Sampling depth (m TOC)	Type of drilling	Casing above ground (m)	Static water level (m TOC)	Sampling depth (m TOC)	Thickness of unconsolidated sediments (m)
F1	2013-10-01	49.68	7.4	Diamond	0.815	1.86	7.5	2.44
F2	2013-10-15	52.12	21.5	Diamond	0.660	2.76	21.5	6.1
F3	2013-10-30	50.00	22.7 (shallow) 50.0 (deep)	Diamond	0.800	1.68	22.7	20.12
F4	2013-11-04	60.35	54.0	Diamond	1.050	8.87	54	40.84
F5	2014-09-15	51.82	14.4	Hammer	0.940	2.30	14.4	9.75
F6	2014-09-17	51.82	10	Hammer	1.005	2.35	10	6.71
F7	2014-10-21	51.51	17.7 (shallow) 48.0 (deep)	Diamond	0.820	4.42	17.7	11.43
F8	2014-10-23	51.51	20.2	Diamond	0.800	0.72	20.2	1.43
F10	2014-09-16	30.48	23.8	Hammer	0.815	3.84	23.8	15.85
F11	2014-09-16	54.86	16.0	Hammer	0.580	2.60	10.3	6.4
F12	2014-09-18	73.15	20.4	Hammer	1.010	3.02	20.4	7.92
F13	2014-09-18	60.96	7.7	Diamond	0.970	2.13	7.7	1.83
F14	2014-09-22	30.48	Dry	Hammer	0.406	30.92	nd	nd
F20	2014-10-01	49.99	7.4 (shallow) 48.5 (deep)	Diamond	0.930	0.73	7.4	3.05
F21	2014-10-06	147.53	31.0 (shallow) 146.7 (deep)	Diamond	0.000	3.60	145	3.05

Hammer : hammer-drilled

Diamond : diamond-drilled

m TOC : meters from top of casing

- The Utica Shale in southern Quebec is known to contain important quantities of gas
- A baseline groundwater study is presented for a 500-km^2 area around St-Edouard, Qc.
- Methane (CH_4) was detected in 96% of the 48 sampling points
- CH_4 concentrations in samples vary between undetected (<0.006 mg/L) and 82 mg/L
- CH_4 distribution is mainly related to geology, water chemistry and flow conditions